Doping the chiral spin liquid: Topological superconductor or chiral metal

Xue-Yang Song, Ashvin Vishwanath, and Ya-Hui Zhang
Department of Physics, Harvard University, Cambridge, Massachusetts 02138, USA

(Received 29 January 2021; revised 4 April 2021; accepted 6 April 2021; published 27 April 2021)

We point out that there are two different chiral spin liquid states on the triangular lattice and discuss the conducting states that are expected on doping them. These states labeled CSL1 and CSL2 are associated with two distinct topological orders with different edge states, although they both spontaneously break time reversal symmetry and exhibit the same quantized spin Hall conductance. While CSL1 is related to the Kalmeyer-Laughlin state, CSL2 is the $\nu = 4$ member of Kitaev's 16-fold way classification. Both states are described within the Abrikosov fermion representation of spins, and the effect of doping can be accessed by introducing charged holons. On doping CSL2, condensation of charged holons leads to a topological $d + id$ superconductor. However on doping CSL1, in sharp contrast, two different scenarios can arise: first, if holons condense, a chiral metal with enlarged unit cell and finite Hall conductivity is obtained. However, in a second novel scenario, the internal magnetic flux adjusts with doping and holons form a bosonic integer quantum Hall state. Remarkably, the latter phase is identical to a $d + id$ superconductor. In this case the Mott insulator to superconductor transition is associated with a bosonic variant of the integer quantum Hall plateau transition. We connect the above two scenarios to two recent numerical studies of doped chiral spin liquids on a triangular lattice. Our work clarifies the complex relation between topological superconductors, chiral spin liquids, and quantum criticality.

DOI: 10.1103/PhysRevB.103.165138

I. INTRODUCTION

Ever since Anderson conceived of the resonating-valence-bond (RVB) liquid as a precursor state to the superconductor in the cuprates [1], the notion of quantum spin liquids (QSLs) has been inextricably tied to mechanisms for high-temperature superconductivity. A considerable body of work has explored doping spin liquid or Mott insulators [2–21]. In referring to QSLs, it is customary to describe them in terms of two features: the emergent gauge group, e.g., Z_2 and U(1) spin liquids and additionally the statistics of "spinon" excitations carrying spin 1/2 and gauge charge. Here we will consider the case of fermionic spinons [22,23]. A Mott insulator to superconductor transition upon doping is quite natural when the parent Mott insulator is a Z_2 spin liquid [2]. Note, a Z_2 spin liquid can be described by a parton mean field ansatz with fermionic spinons in a Bardeen- Cooper-Schrieffer (BCS) state. Doped charges are accounted for in terms of bosonic holons, which can condense. Holon condensation makes the pairing of spinons evolve into true Cooper pairs of electrons, leading to a superconducting phase. In contrast, doping a $U(1)$ spin liquid with a spinon Fermi surface naturally gives us a Fermi liquid phase, rather than a superconductor, because there is no pairing of spinons in the parent Mott insulator [24].

This brings us to the subject of this paper, the chiral spin liquid (CSL) [25,26], and the conducting states that emerge on doping. Chiral spin liquids spontaneously break time reversal symmetry and exhibit chiral edge modes. In particular, a speculative connection between fractional statistics that exist in chiral spin liquids and two-dimensional superconducting states, so-called anyon superconductivity, has been studied in the earlier days of high-T_c superconductivity [26–30]. Theoretically, chiral spin liquids have been found to be the ground state for various spin-1/2 lattice models on the kagome and triangular lattices [31–40] and also in $SU(N)$ model with $N > 2$ [41–44]. On the experimental side, recent observation of a quantized thermal Hall effect in a Kitaev material [45] suggests a non-Abelian chiral spin liquid. These examples motivate us to ask: what is the fate of a chiral spin liquid on doping? Surprisingly we find that this question is more complicated and potentially also more interesting than the usual situation of simple Z_2 spin liquid, where the conventional RVB theory works well.

The first complexity is that there are actually two different chiral spin liquids: CSL1 and CSL2 [46]. CSL1 is an analog of the fractional quantum Hall state in a spin system, as proposed by Kalmeyer-Laughlin [25] and later found to be realized by certain microscopic spin Hamiltonians [47–50]. In contrast, CSL2 should be thought as a "gauged" chiral superconductor, whose wave function is obtained by Gutzwiller projection of a spin singlet superconductor with $d_{x^2-y^2} + id_{xy}$ superconducting pairing, abbreviated as $d + id$ pairing [46,51]. Both CSL1 and CSL2 can be conveniently described using a mean field ansatz of Abrikosov fermions, generically not gauge equivalent to each other. For CSL1, the fermionic spinons are put in a Chern insulator phase with $C = 2$. In contrast, the spinon is in a $d + id$ superconductor ansatz in the CSL2, very similar to a Z_2 spin liquid in terms of wave function. Hence the conventional RVB theory can be generalized to this case and a $d + id$ superconductor naturally emerges from doping. A dual viewpoint involves beginning in the $d + id$ superconductor, and driving a superconductor-insulator transition by condensing pairs of vortices [52], leading directly to CSL2.

 ©2021 American Physical Society

On the other hand, the wave function of CSL1 is a Gutzwiller projection of Chern insulator. Thus a superconductor is not expected from the RVB picture. As far as we know, all of the chiral spin liquids found in numerics for spin rotation invariant spin- 1/2 model are CSL1 [31–34,39,40]. This strongly suggests CSL1 as a more likely candidate relevant to realistic spin-1/2 materials. Then a natural question that arises is: what should we expect on doping this chiral spin liquid?

The main result of this paper is to propose two different scenarios for doping CSL1 on the triangular lattice. In the first scenario, a simple generalization of RVB theory using slave boson condensation [2] predicts a doped Chern insulator. On a triangular lattice, this is a chiral metal with doubled unit cell and staggered loop current order. It also breaks the C_6 rotation symmetry completely and has a nonzero electrical Hall conductivity. This is well described by a mean-field theory of electrons, which basically inherits the mean-field ansatz of spinons in the Mott insulator. An unconventional second possibility is a $d + id$ superconductor emerges from a completely different mechanism, which cannot be captured by simple mean field theory. The doped holon forms a bosonic state with an integer quantum Hall(bosonic-IQH) effect [53,54]. The bosonic holons lead to an opposite Hall conductivity ($\sigma^b_{xy} = -2$) compared to the fermionic spinons. The final wave function of an electron is a product of a bosonic IQH state and a fermionic IQH state. This construction, surprisingly, turns out to describe a superconductor with the same topological property as the $d + id$ superconductor as we will show below.

Our proposed two scenarios for doping CSL1 are in agreement with with two recent numerical studies of a doped chiral spin liquid on triangular lattice. Reference [55] finds a $d + id$ superconductor from doping a CSL in the strong Mott regime described by a $J_1 - J_2 - J_\chi$ model [56,57]. In contrast, Ref. [58] observes a chiral metal phase upon doping a CSL in the weak Mott regime [39]. The CSLs in the parent Mott insulators in the above two cases are shown to be both the CSL1 because the measured entanglement spectrum is consistent with the $SU(2)_1$ edge theory [39,56]. Lastly we note that there are other numerical studies of possible superconductivity on a triangular lattice where the parent state is not a chiral spin liquid [15,21,59]. Further work will be needed to synthesize these observations into a coherent theory. However, it is clear that there are at least two competing phases upon doping the same CSL, which is consistent with the framework in our paper.

II. TWO CHIRAL SPIN LIQUIDS ON TRIANGULAR LATTICE

We adopt a parton construction to decompose the physical electron operator as a boson carrying its electric charge (called holon) and a fermionic spinon carrying spin indices:

$$c_{i,\sigma} = b_i^\dagger f_{i,\sigma}, \tag{1}$$

where σ, i denote spin and site, respectively. This formalism introduces a $U(1)$ gauge redundancy between the holon and spinon, with a $U(1)$ gauge field a. Hence it leads to a gauge constraint $n_i^b + n_i^f = 1$. Note that there is an $SU(2)$ version of the parton construction with two slave bosons per site [2] reviewed in Appendix A and for our purpose the above $U(1)$ partons suffice.

At integer filling $n_i = 1$, the holons are trivially gapped and the mean field for spinons is conveniently written in the basis $\psi_i = (f_{i,\uparrow}, f_{i,\downarrow}^\dagger)^T$, with Pauli matrices $\tau^{x,y,z}$ acting in such a spinor space:

$$\mathcal{H}_{\text{spinon}} = \sum_{\langle ij\rangle} \psi_j^\dagger u_{i,j} \psi_i, \tag{2}$$

where one considers only nearest neighbor terms. u's are 2×2 matrices, satisfy $u_{i,j} = u_{j,i}^\dagger$ and contain hopping and pairing as diagonal, off-diagonal elements, respectively. We use coordinates shown at upper right of Fig. 2.

There are two kinds of chiral spin liquid variational states that break time reversal and mirror symmetry on triangular lattices that have been extensively studied: the $U(1)_2$ chiral spin liquid (CSL1) and the projected $d + id$ superconductor (CSL2). Below we review the mean field theory for the two states and discuss their connection and differences.

A. CSL1: $U(1)_2$ chiral spin liquid

The $U(1)_2$ chiral spin liquid, which we study in this paper, is described by a Chern insulator of the spinons with total Chern number (combining the two spins) $C = 2$. Typical realizations consist of a π hopping flux of each spinon f_σ through a rhombus of the triangular lattice, with the flux $\pi/2 \pm 3\theta$ around an upward and downward triangle for the spinon. This staggered-flux ansatz typically gives a gapped dispersion for each spinon species, forming two Chern bands with $C = \pm 1$; at the point $\theta = \pm\pi/6$, the dispersion becomes gapless and a Dirac spin liquid (DSL) emerges [60]. The mean-field ansatz of spinon hopping reads

$$\begin{aligned} u_{r,r+\hat{x}} &= ie^{i(\frac{\pi}{2}+\theta)\tau^z}, \\ u_{r,r+\hat{y}} &= (-1)^{r_x} ie^{i(\frac{\pi}{2}+\theta)\tau^z}, \\ u_{r,r+\hat{x}+\hat{y}} &= (-1)^{r_x} ie^{-i\theta\tau^z}, (\theta \in (-\pi/3, \pi/3)), \end{aligned} \tag{3}$$

where the x, y coordinates are shown in Fig. 2. In this gauge choice, the lower spinon band hits the lowest energy at zero momentum and the highest energy at momenta $(\pi/3, \pi/3)$, $(4\pi/3, -2\pi/3)$, independent of θ. See Fig. 1 for the dispersion of the spinon bands for various θ values.

$\mathcal{H}_{\text{spinon}}$ as in Eq. (3) is invariant under a projective translation and sixfold rotation symmetries, while breaking time reversal and mirror symmetry except at the special point $\theta = \pm\pi/6$. The projective symmetry group for the spinons reads

$$\begin{aligned} &T_x : \psi_r \to (-1)^{r_y} \psi_{r+\hat{x}}, \\ &T_y : \psi_r \to \psi_{r+\hat{y}}, \\ &C_6 : \psi_r \to \begin{cases} \tau^x \psi_{C_6 r} & (C_6 r)_y \mod 2 = 0 \\ -(-1)^{(C_6 r)_x} i\tau^x \psi_{C_6 r} & (C_6 r)_y \mod 2 = 1 \end{cases}, \end{aligned} \tag{4}$$

where $C_6 r$ is the C_6 rotated position of the site at r.

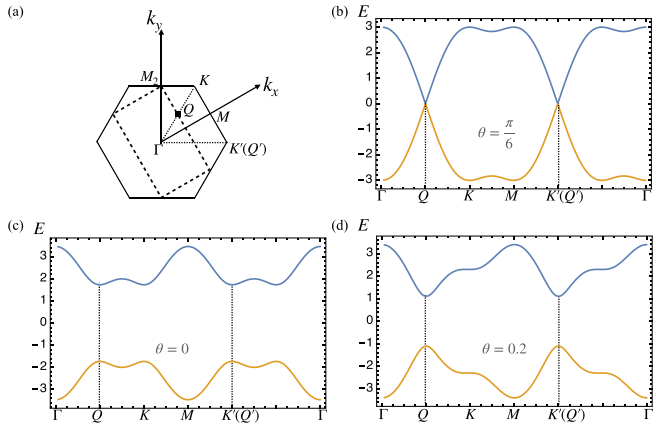

FIG. 1. Dispersion of spinons for $\mathcal{H}_{\text{spinon}}$ in Eq. (3).The band is particle-hole symmetric. (a) The original (reduced) hexagonal (square, dashed) Brillouin zone and the dispersion plots are along the loop $\Gamma \to K \to K' \to \Gamma$ where $\mathbf{Q} = (\pi/3, \pi/3)$, $\mathbf{Q}' = (4\pi/3, -2\pi/3)$ are points of maximal energy in the valence band. Γ, M_2 are points of lowest energy in valence band. (b) The dispersion at the DSL gapless point $\theta = \pi/6$. (c),(d) Dispersions at $\theta = 0, 0.2$, respectively. The Chern number of valence (conduction) bands is $C = \pm 1$.

The low-energy physics of the CSL1 is captured by the following action:

$$L = -\frac{1}{4\pi}\alpha_1 d\alpha_1 - \frac{1}{4\pi}\alpha_2 d\alpha_2 + \frac{1}{2\pi} a d(\alpha_1 + \alpha_2) + \frac{1}{2}\frac{A_s}{2} d(\alpha_1 - \alpha_2), \tag{5}$$

where A_s is the external spin field in the convention that its charge $q_s = \frac{1}{2}$ for $S_z = \frac{1}{2}$. α_1, α_2 are introduced to represent the IQH of $f_\uparrow$ and $f_\downarrow$ respectively. a is the internal $U(1)$ gauge field shared by the slave boson b and the spinon f_σ.

We can also integrate a to lock $\alpha_1 = -\alpha_2 = \alpha$, then we get

$$L = -\frac{2}{4\pi}\alpha d\alpha + \frac{1}{2\pi} A_s d\alpha. \tag{6}$$

This is a $U(1)_2$ theory which also describes the $\nu = \frac{1}{2}$ Laughlin state. Exploiting the relation between spin-1/2 and hard core bosons, one can map the $\nu = \frac{1}{2}$ Laughlin state of boson to a spin state, which corresponds to CSL1. Thus the CSL1 has the same topological order as the $\nu = \frac{1}{2}$ Laughlin state. Indeed a model wave function using the Laughlin state was proposed by Kalmeyer-Laughlin [25]. But we need to emphasize that a general state with any $\theta \neq \pm\frac{\pi}{6}$ is in the same topological phase as the Kalmeyer-Laughlin state. There are two anyons in this phase: I and s, with s as a spin-1/2 semion. The edge state is characterized by chiral central charge $c = 1$.

B. CSL2: Projected $d + id$ superconductor

The projected $d + id$ superconductor is given by the u matrices below:

$$u_{r,r+\hat{x}} = \frac{1}{\sqrt{\chi^2 + \eta^2}}(\chi\tau^z + \eta\tau^x),$$

$$u_{r,r+\hat{y}} = \frac{1}{\sqrt{\chi^2 + \eta^2}}\left[\chi\tau^z + \eta\left(\tau^x \cos\frac{4\pi}{3} - \tau^y \sin\frac{4\pi}{3}\right)\right],$$

$$u_{r,r+\hat{x}+\hat{y}} = \frac{1}{\sqrt{\chi^2 + \eta^2}}\left[\chi\tau^z + \eta\left(\tau^x \cos\frac{2\pi}{3} - \tau^y \sin\frac{2\pi}{3}\right)\right], \tag{7}$$

with χ, η as real parameters and explicit translation invariance. The pairings for 3 bonds generated by C_3 rotation have phases $0, 2\pi/3, 4\pi/3$ respectively, the same as that of a $d + id$ superconductor.

The topological order depends on the angular momentum of the corresponding pairing, as classified by Kitaev's 16-fold way [61]. With $SU(2)$ spin rotation symmetry, the pairing can only be in the even angular momentum channel, making the gauged $d + id$ superconductor as the simplest chiral spin liquid in the CSL2 category. There are four anyons labeled by $1, e, m, \epsilon$ in CSL2 [62]. e, m are semions with $\pi/2$ self-statistics and trivial mutual statistics. ϵ is a bound state of e, m and has fermionic statistics. This state corresponds to $\nu = 4$ of Kitaev's 16-fold classification of Z_2 topological order [61] and its topological order is $U(1)_2 \times U(1)_2$. Its edge theory has chiral central charge $c = 2$. The wave function of CSL2 is a Gutzwiller projection of a $d + id$ superconductor instead of an s-wave superconductor.

C. Relation between two CSLs

We note that these two CSL states generically are not equivalent, since the invariant gauge group (IGG) for projected $d + id$ states (CSL2) is Z_2, while IGG for CSL1 is $U(1)$. Moreover, they differ in the topological orders and anyon contents as described above.

We note however the following collision between these two ansatz and clarify its meaning. For CSL2, at the special point when $\eta = \sqrt{2}\chi$, the Wilson loop around one triangle for projected $d + id$ reads $\Phi = u_{r,r+\hat{x}} u_{r,r+\hat{y}} u_{r,r-\hat{x}-\hat{y}} \propto i\tau^0$, equivalent to that of the CSL1 at $\theta = 0$. Hence the two states are gauge equivalent at the special point. Specifically, there is an $SU(2)$ gauge transform g_r which rotates the mean-field ansatz for CSL1 (3) at $\theta = 0$ to the mean-field $d + id$ ansatz of CSL2 Eq. (7) at $\eta = \sqrt{2}\chi$:

$$\psi_r \to g_r \psi_r,$$

$$g_r = \begin{cases} 1 & r_x \text{ even}, r_y \text{ even} \\ -\frac{\tau^z + \sqrt{2}\tau^x}{\sqrt{3}} & r_x \text{ odd}, r_y \text{ even} \\ \frac{-(\tau^z + \sqrt{2}(\tau^x \cos\frac{4\pi}{3} - \tau^y \sin\frac{4\pi}{3}))}{\sqrt{3}} & r_x \text{ even}, r_y \text{ odd} \\ \frac{-i(\tau^z + \sqrt{2}(\tau^x \cos\frac{2\pi}{3} - \tau^y \sin\frac{2\pi}{3}))}{\sqrt{3}} & r_x \text{ odd}, r_y \text{ odd}. \end{cases} \tag{8}$$

At the special point $\theta = 0$, the IGG is actually enlarged to $SU(2)$ and the low energy theory is $SU(2)_1$, which is known to be equivalent to the $U(1)_2$ theory. Hence the special point with $\theta = 0$ also belongs to the CSL1. At the same time, the point $\eta = \sqrt{2}\chi$ does not belong to CSL2, since the gauge group is enlarged to $SU(2)$. However, on moving away from this special point, a Higgs condensate develops, lowering the gauge group to Z_2.

One can ask what the gauge transformation above accomplishes when θ shifts away from 0 for CSL1 ansatz. Then the above rotation Eq. (8) on the CSL1 does not restore explicitly lattice translation as present in the $d + id$ ansatz (see Appendix B. The transformed state at $\theta \neq 0$ has $d + id$ pairing, but breaks translation symmetry and despite the fact that it appears to be a pairing state, it secretly possesses a $U(1)$ IGG.

III. CHIRAL METAL

At hole doping level x, the average density of the holon and the spinon per site becomes $n_i^b = x$ and $n_i^f = 1 - x$. One simple possibility is that the slave boson condenses at zero temperature. This is obtained self-consistently for a mean-field ansatz of holons. Assuming an electron hopping term in the parent Hubbard model of the form $H_{KE} = -t \sum_{\langle ij \rangle} c_{i\sigma}^\dagger c_{j\sigma} + \text{h.c.}$ with real $t > 0$, we can obtain the mean-field theory of the holon as

$$\mathcal{H}_{\text{holon}} = t \sum_{\langle ij \rangle, \sigma} \langle f_{i,\sigma} f_{j,\sigma}^\dagger \rangle b_i^\dagger b_j, \tag{9}$$

where $\langle f_{i,\sigma} f_{j,\sigma}^\dagger \rangle$ is computed on the ground state of the spinon mean field $\mathcal{H}_{\text{spinon}}$ and is proportional to spinon hopping terms on corresponding bonds. The lowest energy states for $\mathcal{H}_{\text{holon}}$ lie at Γ, M_2 momenta, and hence holon condensation is generically a superposition of these two states. The favored condensation is given by optimizing the kinetic energy of electrons in H_{KE},

$$E_{KE} = t \sum_{\langle ij \rangle, \sigma} \langle f_{i,\sigma} f_{j,\sigma}^\dagger \rangle \langle b_i^\dagger \rangle \langle b_j \rangle, \tag{10}$$

where the holon condensed values

$$\langle b_i \rangle = \sqrt{2x}[p_\Gamma u_\Gamma(i_s) + (1 - p_\Gamma)(-1)^{i_y} u_{M2}(i_s)], \tag{11}$$

where $p_\Gamma \in [0, 1]$ is the fraction of holons that condense at Γ. $u_{\Gamma,M2}(i_s = A, B)$ are the Bloch wave functions at Γ, M_2 momenta on two sublattices,

$$\begin{aligned} u_\Gamma(A) &= 0.63(1 + i), u_\Gamma(B) = 0.46, \\ u_{M2}(A) &= 0.33(1 - i), u_{M2}(B) = 0.89, \end{aligned} \tag{12}$$

identically for any θ.

We found that for negative hopping in H_{KE}, the holons fully condense at $M_2 = (0, \pi)$ to optimize the kinetic energy, i.e., $p_\Gamma = 0$ in Eq. (11). This is true for any $\theta \in (-\pi/6, \pi/6)$. For positive hopping (or equivalently doping electrons), holons fully condense at Γ, i.e., $p_\Gamma = 1$. The wave functions with minimal energy for $-\mathcal{H}_{\text{holon}}$ read

$$\begin{aligned} \tilde{u}_\Gamma(A) &= 0.33(-1 - i), \tilde{u}_\Gamma(B) = 0.89, \\ \tilde{u}_{M2}(A) &= 0.63(-1 + i), \tilde{u}_{M2}(B) = 0.46. \end{aligned} \tag{13}$$

Holon condensation leads to the electron operator as

$$c_{i,\sigma} = \langle b_i^\dagger \rangle f_{i,\sigma}. \tag{14}$$

Spinons are away from integer filling upon doping and states at the valence band top are emptied as Fermi pockets. Electrons, identified as spinons in Eq. (14) hence partially fill states in a band and form a metal with π flux and breaks translation, rotation and time reversal, as the spinon Hamiltonian

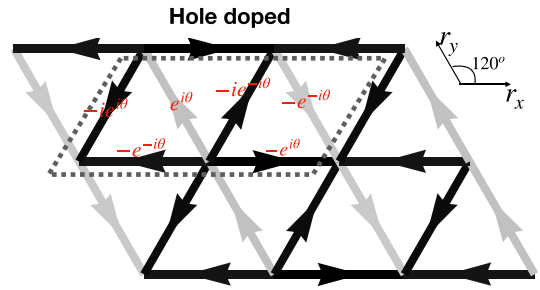

FIG. 2. A doubled unit cell shown in dotted parallelogram. Spinon hopping ansatz of the CSL shown in red on the bond inside the dotted parallelogram, direction in line with arrows on bonds. The relative current strength $I_{\text{bond}\langle ij \rangle} = \text{Im}[c_i^\dagger c_j]$ of the chiral metal upon infinitesimal doping of holes ($\theta = 0$) shown schematically by the bond gray level (the smaller the current is, the grayer the bond looks) with arrows indicating current directions. The currents are given by holon condensation at Γ, M_2 momenta such that the kinetic energy of electrons $-t \sum_{\langle ij \rangle} c_i^\dagger c_j$ is optimized. For doping holes, holons fully condense at M_2 and the currents have a *doubled* unit cell structure. For doping electrons, currents are opposite to those in the hole scenario.

does. Numerically, we found a nonvanishing bond current pattern of the metal $I_{\text{bond}\langle ij \rangle} \equiv \text{Im}[c_i^\dagger c_j]$ shown in Fig. 2 (parameter $\theta = 0$), at infinitesimal doping.

For the electron doping scenario, one changes the parton definition to $c_{i,\sigma}^\dagger = b_i^\dagger f_{i,\sigma}$, which corresponds to a particle-hole transformation for the electrons, and hence results in a minus sign multiplying the hopping amplitude $-t$ in H_{KE}. To optimize $-H_{KE}$, holons all condense at Γ, currents are opposite to the hole doping scenario shown in Fig. 2, up to a $\widehat{r}_x$ translation of y bond currents. We also present the current patterns at $\theta = \pm 0.2, \pm 0.4$ upon infinitesimal hole doping in supplementary Fig. 8 with holons condensing fully at Γ.[1] The current pattern generically holds a 2×2 unit cell due to holons condensing at both Γ, M_2 when going beyond a mean-field treatment; only when holons condense solely at Γ or M_2 does it yield a 2×1 unit cell pattern.

The electrons have a nonvanishing Hall response as the spinons are in a Chern band. From the Ioffe-Larkin rule, one has for the resistivity tensors $\rho_c = \rho_b + \rho_f$ where $\rho_b = 0$ identically since holons have condensed. At small doping, $\rho_c = \rho_f$. Note that when holons condense, an extra term appears for the spinon mean field after substituting electron operators from Eq. (14)

$$\overline{\mathcal{H}_{\text{spinon}}} = \mathcal{H}_{\text{spinon}} - \sum_{\langle ij \rangle, \sigma} t \langle b_i \rangle \langle b_j \rangle^* f_{i,\sigma}^\dagger f_{j,\sigma}, \tag{15}$$

which should be small when light doping and we ignored such terms. For a free fermion system σ_{xy} is given by the Kubo

[1]In numerics, the relative strength of the current may change by as much as 0.08 (normalized by the strongest current), when increasing the density of momenta used for calculations, from a density of 400 points per unit area to 10 000 points per unit area.

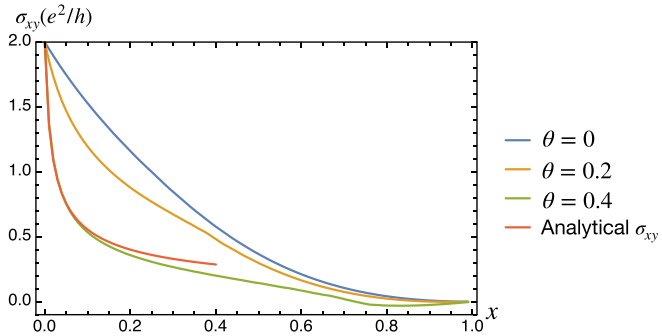

FIG. 3. The numerical hall conductivity σ_{xy} of the chiral metal upon doping holes at fractions x at selected values $\theta = 0, 0.2, 0.4$, respectively. The results are expected to be accurate for light doping. The red line is the analytical expression for σ_{xy} Eq.(17) for $\theta = 0.4$, near the gapless point $\theta = \pi/6$. It fits well with the numerical results at small doping $x < 0.1$. σ_{xy} in the electron doping scenario is identical to that of the hole-doping case at same doping level x.

formula as

$$\sigma_{xy} = \frac{e^2}{\hbar}\int_{E_k<\epsilon_f}\frac{d^2k}{4\pi^2}2\mathrm{Im}\left[\left\langle\frac{\partial u}{\partial k_1}\middle|\frac{\partial u}{\partial k_2}\right\rangle\right], \tag{16}$$

where $u(k_1, k_2)$ is the periodic Bloch wave function for $\mathcal{H}_{\text{spinon}}$ and the integration is over filled states. See Appendix D for numerical details on calculating Berry curvatures. Figure 3 shows the hall conductivity σ_{xy} as one varies hole doping fraction x and hopping phase θ. It extrapolates to the quantized value of $2e^2/h$ at zero doping. The Hall conductivity upon doping electrons, meanwhile, is identical to that on the hole side of the same doping level x.

Near the gapless point $\theta = \pm\pi/6$, one could approximate states near the valence band top as Dirac fermions with a chiral mass, and analytically (see Appendix D) express the Hall conductivity by integrating Berry curvatures of filled states, i.e., the Hall conductivity as a function of $\Delta = |\pi/6 - \theta|, x$ reads

$$\sigma_{xy}(x, \Delta) = \frac{4\sqrt{3}\Delta}{\sqrt{12\Delta^2 + 4\sqrt{3}\pi x}}. \tag{17}$$

The enlarged unit cell implies a density wave formation in the chiral metal where states at $\mathbf{k}$ and $\mathbf{k} + \mathbf{G}_1$ couple together, where $\mathbf{G}_1 = (\pi, 0)$ is a reciprocal vector for the reduced Brillouin zone (BZ) ($2\mathbf{G}_1$ for the original hexagonal Brillouin zone). Figure 4 presents numerical results on the spectral function $A(\mathbf{k}, \omega = 0) = 2Im[G_R(\mathbf{k}, \omega = i0^+)]$ where G_R is the retarded Green's function, as measured by angle-resolved photo emission spectroscopy (ARPES). Details of calculation are shown in Appendix E. The duplication of Fermi surfaces separated by $\mathbf{G}_1$ is a signature of the density wave.

In the previous discussion we determine the ansatz of the spinon f and the wave function of the holon $\langle b_i\rangle = \mu_i$ through mean-field calculation. In practice, one can also apply the variational Monte Carlo technique to determine these parameters by studying the following model wave function:

$$\Psi(x_1, \ldots, x_N) = P_G\left(\prod_i \mu_i^{1-n_i}\right)\text{Slater}[x_1, \ldots, x_N], \tag{18}$$

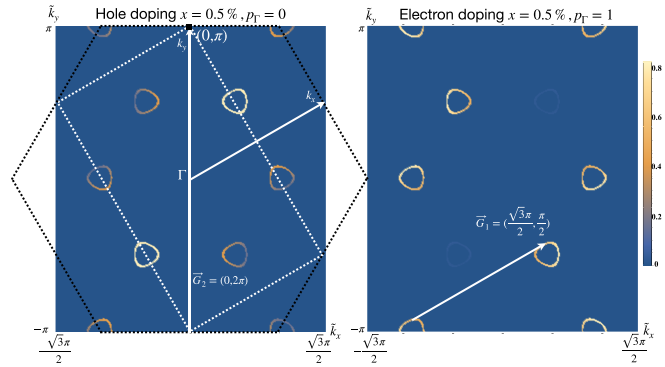

FIG. 4. The numerical results for spectral function for the chiral metal at zero frequency $A(\mathbf{k}, \omega = 0) = 2\mathrm{Im}[G_R(\mathbf{k}, \omega = i0^+)]$(a.u.), where the retarded Green's function $G_R(\mathbf{k}, \omega) = \int_0^\infty \frac{dt}{2\pi} e^{i\omega t}\langle[c_k^\dagger(t), c_k(0)]\rangle_{GS}$, at $\theta = 0$ and doping level marked at the top. The left(right) panel shows the case for hole(electron) doping with $p_\Gamma, 1 - p_\Gamma$ of holons condensing at Γ, M_2, respectively. The spectral function could be measured as in ARPES, where the absolute momenta in the original Brillouin zone(black dotted hexagonal) are resolved. The Fermi surface is duplicated after a translation of $\mathbf{G_1}$(coordinates written in $\tilde{k}_x - \tilde{k}_y$ basis) corresponding to the reciprocal vector of the reduced BZ (white dotted square in the left panel).

where Slater is a Slater determinant according to the mean-field ansatz of the spinon f. P_G is the usual Gutzwiller projection to forbid the double occupancy. Here we introduce $\langle b_i\rangle = \mu_i$ as variational parameters. In practice one can focus only on a 2×2 unit cell and hence there are four complex parameters for μ_i.

The CSL1 with $\theta = 0$ needs special treatment. At this special point, the spinon ansatz is gauge equivalent to a $d + id$ superconductor. Thus a translation invariant $d + id$ superconductor is also possible upon doping. However, there is no reason to expect that a CSL1 state is fine tuned to be at $\theta = 0$. For example, CSL1 found in $J_1 - J_2 - J_\chi$ model [56] is believed to be close to a Dirac spin liquid at $J_\chi = 0$ line. Thus the spinon ansatz should be a Dirac spin liquid with small chiral mass, for which θ should be close to $\frac{\pi}{6}$. For generic θ, a translation invariant $d + id$ superconductor is not possible in the picture of holon condensation.

A comparison with doping square lattice CSL is in order: On the square lattice, there are also two different CSL: CSL1 and CSL2 as on a triangular lattice. But for a square lattice, the ansatz of spinons for CSL1 can always be written in the form of $d + id$ superconductor (without hopping on the next nearest neighbor) (please see Appendix. C). In this case, doping can lead to a translation invariant $d + id$ or a chiral metal, depending on which one is energetically favorable. This is different from a triangular lattice where only a special point of CSL1 has spinons in a $d + id$ superconductor ansatz.

IV. TOPOLOGICAL SUPERCONDUCTOR FROM DOPING THE GENERIC KALMEYER-LAUGHLIN SPIN LIQUID CSL1

From the Z_2 spin liquid, RVB theory predicts a superconducting phase upon doping. One natural question is: can we also get a superconductor from doping a chiral spin liquid.

For CSL2, this is obvious as the spinons are already in a BCS state. For the CSL1, the focus here, it is not obvious how to do this except at the special point $\theta = 0$. At a generic point with $\theta \neq 0$, there is no gauge transformation which can make the spinon ansatz into a translation invariant $d + id$ superconductor. There is a particular gauge in which spinons are in a translation symmetry *breaking* superconductor, as shown in Appendix B However, in numerics the $d + id$ superconductor that emerges from doping a CSL1 is found to be translationally invariant [55]. This result therefore cannot be explained by the conventional RVB picture and requires a new theory. In the following we propose precisely such an exotic mechanism for obtaining a topological superconductor from doping the Kalmeyer-Laughlin CSL1.

We first turn to the slave boson theory $c_{i;\sigma} = b_i f_{i;\sigma}$ with the constraint $n_i^b = n_i^f$. The slave boson b and the spinon f now have opposite gauge charges. At zero doping, there is an internal flux $\Phi = \pi$ per unit cell and the effective filling in terms of the magnetic flux for b and f are $\nu_b = -2$ and $\nu_f = 2$, respectively. For the CSL, f is in the $C = 2$ Chern insulator, while the slave boson b is in a trivial Mott insulator with one particle per site. When we decrease the Hubbard U or change the doping, the slave boson b can not be in a Mott insulator anymore and will delocalize after a Mott transition. The usual story is that the slave boson will just condense, which in our case leads to a Chern insulator at zero doping and chiral metal at finite doping. However, as the slave boson is at filling $\nu_b = -2$ in terms of the magnetic flux, there is another option after the Mott transition: the slave boson can be in a quantum Hall liquid phase instead of a superfluid phase. The most natural choice is the bosonic integer quantum Hall (bIQH) state, which has been found numerically in the lattice model with flux $\Phi = \pi$ per unit cell [63]. As we show later, the resulting phase turns out to be a topological superconductor in the same class of $d + id$ superconductor. The easiest way to see the superconductivity is through the Ioffe-Larkin rule: the resistivity tensor of an electron is $\rho_c = \rho_b + \rho_f$, where ρ_b, ρ_f are the resistivity tensor for b and f. As b and f are in quantum Hall phase with opposite Hall conductivity, $\rho_c = \left(\begin{smallmatrix} 0 & -2 \\ 2 & 0 \end{smallmatrix}\right) + \left(\begin{smallmatrix} 0 & 2 \\ -2 & 0 \end{smallmatrix}\right) = \left(\begin{smallmatrix} 0 & 0 \\ 0 & 0 \end{smallmatrix}\right)$, which describes a superconductor.

A superconductor phase obviously should survive when changing the doping. To keep it in a superconductor phase, we need both b and f in the quantum Hall phase even after doping. At finite doping x, it turns out that the internal magnetic flux needs to adjust itself to

$$\Phi(x) = \frac{\langle da \rangle}{2\pi} = \frac{1-x}{2}. \tag{19}$$

In the language of projective symmetry group (PSG) this means that b and f are obeying a magnetic translation symmetry: $T_1 T_2 = T_2 T_1 e^{\pm i 2\pi \Phi(x)}$, where $\pm$ arises because b and f carry opposite gauge charges. The electron $c = bf$, however, still satisfies the usual translation symmetry because the phase factors from b and f cancel each other. We believe that the final electron phase is translation invariant.

The lock of the internal flux to the additional doping keeps the spinon f in the $C = 2$ Chern insulator phase and b in the bIQH phase according to the Streda formula at arbitrary doping level x. The final wave function is a product of two quantum Hall wave functions:

$$\Psi(\mathbf{x}_1, \ldots, \mathbf{x}_N) = P_G \Psi_{\mathrm{bIQH}}(\mathbf{x}_1, \ldots, \mathbf{x}_N) \Psi_{\mathrm{fIQH}}(\mathbf{x}_1, \ldots, \mathbf{x}_N), \tag{20}$$

where Ψ_{bIQH} is the wave function of the bIQH state at $\nu = -2$ and Ψ_{fIQH} is the wave function of a fermionic IQH state with $\nu = 2$. P_G is the usual Gutzwiller projection to forbid double occupancy. A concrete wave function of Ψ_{bIQH} based on a mean-field ansatz can be found in Appendix F 3.

One can see that this model wave function is quite distinct from the usual RVB wave function. In our wave function, none of b and f have pairing structure, but the resulting phase is a superconductor. In the following we study the topological property of this phase more carefully. The low energy theory is

$$L = L_{b,\mathrm{IQH}} + L_{f,\mathrm{IQH}}. \tag{21}$$

We have

$$L_{f,\mathrm{IQH}} = -\frac{1}{4\pi}\alpha_1 d\alpha_1 - \frac{1}{4\pi}\alpha_2 d\alpha_2 + \frac{1}{2\pi} a d(\alpha_1 + \alpha_2) + \frac{1}{2\pi}\frac{A_s}{2} d(\alpha_1 - \alpha_2) \tag{22}$$

and

$$L_{b,\mathrm{IQH}} = \frac{1}{4\pi}\beta_1 d\beta_2 + \frac{1}{4\pi}\beta_2 d\beta_1 + \frac{1}{2\pi}(A_c - a) d(\beta_1 + \beta_2), \tag{23}$$

where we have used the fact that the K matrix for bosonic IQH with $\sigma_{xy} = -2$ is $K = \left(\begin{smallmatrix} 0 & -1 \\ -1 & 0 \end{smallmatrix}\right)$ and the charge vector is $q = (1, 1)^T$. The IQH with $\sigma_{xy} = 2$ for fermion is described by $K = \left(\begin{smallmatrix} 1 & 0 \\ 0 & 1 \end{smallmatrix}\right)$ and charge vector $q = (1, 1)^T$. $\frac{A_s}{2}$ is the spin gauge field. Here we use the convention that $q_s = \pm\frac{1}{2}$ for spin up and down. A_c is the external electromagnetic field and we assign charge to the slave boson b. a is the internal gauge field shared by the slave boson b and spinon f_σ.

We can simplify the action by integrating out a first, which locks $\beta_2 = \alpha_1 + \alpha_2 - \beta_1$. After substitution, we get

$$L = -\frac{2}{4\pi}\beta_1 d\beta_1 - \frac{1}{4\pi}\alpha_1 d\alpha_1 - \frac{1}{4\pi}\alpha_2 d\alpha_2 + \frac{1}{2\pi} A_c d(\alpha_1 + \alpha_2) + \frac{1}{2\pi}\frac{A_s}{2} d(\alpha_1 - \alpha_2) + \frac{1}{2\pi}\beta_1 d(\alpha_1 + \alpha_2). \tag{24}$$

Relabeling $\alpha_c = \frac{\alpha_1+\alpha_2}{2}, \alpha_s = \frac{\alpha_1-\alpha_2}{2}, \beta = -\beta_1 + \frac{\alpha_1+\alpha_2}{2}$, we can rewrite the action as

$$L = -\frac{2}{4\pi}\beta d\beta - \frac{2}{4\pi}\alpha_s d\alpha_s + \frac{1}{2\pi} A_s d\alpha_s + \frac{2}{2\pi} A_c d\alpha_c. \tag{25}$$

We need to emphasize that the quantization of the charge is different from the usual Chern-Simons theory. We have the following dictionary: $q_\beta = -q_{\beta_1}$, $q_c = q_1 + q_2 + q_{\beta_1}$ and $q_s = q_1 - q_2$, where q_{β_1}, q_1, q_2 are the charges of $\beta_1, \alpha_1, \alpha_2$. We require q_{β_1}, q_1, q_2 to be integers to satisfy the usual quantization rule of the Chern-Simons theory. The excitation is labeled by $l = (q_\beta, q_c, q_s)$.

Given that there is no Chern-Simons term for α_c, it represents a gapless charge mode and we have a superconductor.

TABLE I. List of anyons in the topological superconductor. V is the vortex charge. S_z is the spin quantum number and θ is the self statistics. We have $V = q_c$, $S_z = \frac{1}{2}q_s$ and $\theta = \frac{\pi}{2}(q_\beta^2 + q_s^2)$.

	(q_{β_1}, q_1, q_2)	(q_β, q_c, q_s)	θ	S_z	V
I	(0,0,0)	(0,0,0)	0	0	0
e	(0,1,0)	(0,1,1)	$\frac{\pi}{2}$	$\frac{1}{2}$	1
m	$(-1, 0, 0)$	$(1, -1, 0)$	$\frac{\pi}{2}$	0	-1
ϵ	$(-1, 1, 0)$	(1,0,1)	π	$\frac{1}{2}$	0

α_c represents the Goldstone mode and its charge q_c labels the vortex. As the smallest $q_c = q_1 + q_2 + q_{\beta_1}$ is ± 1, the elementary charge of the superconductor is $Q = 2\frac{d\alpha_c}{2\pi} = 2$ and we conclude that it is a charge $2e$ superconductor.

The other excitations are listed in Table I. There are in total four different anyons $1, e, m, \epsilon$, where e and m are two semions and $\epsilon = em$ is a fermion. For each excitaion, we can define two charges. The first one is the spin $S_z = \frac{1}{2}q_s$. The second one is the vortex charge $V = q_c$. The statistics of the anyon is $\theta = \frac{\pi}{2}(q_s^2 + q_\beta^2)$. We find that the two semions e, m always bind with vortex and cost infinite energy. The only finite energy excitation is the fermion ϵ, which can be identified as a Bogoliubov fermion. ϵ has a mutual statistics $\theta_{\epsilon e} = \theta_{\epsilon m} = \pi$ with e, m, consistent with the braiding of the Bogolibov fermion around an elementary vortex. The excitations and their topological properties match that of the $d + id$ superconductor. There is also a spin quantum Hall conductivity $\frac{1}{2}\frac{1}{4\pi}A_s dA_s$, in agreement with the $d + id$ superconductor [64,65]. In summary, we believe the topological property and the symmetry quantum number of the state defined in Eq. (20) is the same as the $d + id$ superconductor.

We comment on similarity and difference from our construction here and a previous theory on doped Dirac spin liquid on a kagome lattice [66]. Both our proposal and that of Ref. [66] needs internal magnetic flux adjusting to the doping. The superconductor proposed in Ref. [66] is not a BCS superconductor and it needs time reversal to be broken only after doping. In our case, there is already an internal magnetic flux breaking time reversal in the Mott insulator and the proposed superconductor is in the same class as a $d + id$ superconductor from BCS theory. Hence our proposal may be easier to be realized in realistic models. Actually, a recent numerical study confirms the existence of a $d + id$ superconductor [55] from doping a CSL1, consistent with our theory.

V. DECONFINED SUPERCONDUCTOR-INSULATOR TRANSITION

In this section we discuss the critical point between the chiral spin liquid Mott insulator and the chiral metal or the topological superconductor. The transition can be tuned by either doping x or via bandwidth control by changing the Hubbard U as shown schematically in Fig. 5. At finite doping, holons may remain in a Mott insulator, i.e., localized by disorder and hence the CSL phase extends to $x \neq 0$ in Fig. 5. Usually the bandwidth controlled or doping controlled Mott transition is described by the condensation of the holons [24].

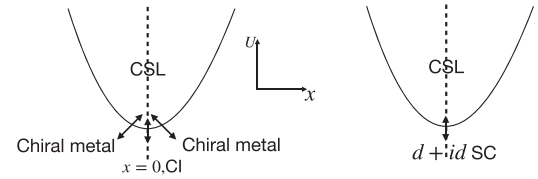

FIG. 5. The schematic phase diagram of the system as a function of interaction strength U and doping level x (positive, negative x denotes doping electrons, holes, respectively). As one decreases U or dopes the system, the CSL may become a chiral metal (left) or $d + id$ superconductor (right), depending on energetics. For the left figure, at exactly $x = 0$ and small U, the system transits to a Chern insulator (CI) with Hall conductivity $\sigma_{xy} = 2$.

The new feature in our theory is the possibility of an unconventional route: the transition into a bIQH insulator for the holons actually closes the Mott gap and makes the electrons into a topological superconductor phase.

The different electron phases associate with different phases of holons, as shown in Fig. 6. Therefore we can reduce the critical theory to the transition between different bosonic phases for the slave boson, similar to the theory in Ref. [24]. The transitions marked by black arrows in the Fig. 6(a) from a trivial gapped state or an IQH state to a superfluid, are described by Bose condensation. The final transition for the corresponding electron phases in Fig. 6(b) needs to further include the gauge field. At zero doping, the chiral metal is really a Chern insulator. In this section we focus on the superconductor insulator transition marked by the red arrow in Fig. 6.

A key component of this superconductor insulator transition is the plateau transition for the slave boson. This transition marked by dotted red arrows from a Mott insulator to bIQH has been studied in Refs. [67–69]. Using a parton construction with six fermionic parton fields (see Appendix F), this transition from Mott to bIQH state happens when one particular parton ψ_1 band's Chern number changes from $C = 1$ to $C = -1$, while other partons remain in some Chern bands. Hence the transition can be described by two Dirac cones $\chi_{1,2}$ in the ψ_1 bands, whose mass sign changes induce changes in the Chern number. We will present the critical theory and analyze its universal property in this section.

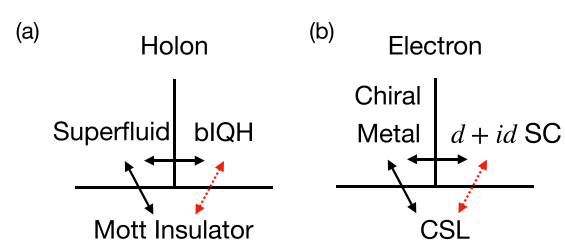

FIG. 6. The possible phases of holons and the corresponding physical phases. The transition of holons from Mott insulators or boson integer quantum hall (bIQH) to superfluid is described by Bose condenstion in $(2 + 1)D$. The direct transition from Mott insulators to bIQH marked by dotted arrows is studied in Sec. V.

A. Critical action and phase diagram

The critical action reads from Appendix F

$$\begin{aligned}\mathcal{L}_{\rm cri} &= \sum_{i=1,2} \bar{\chi}_i \eta_\mu (i\partial_\mu + A_{c,\mu} + \gamma_\mu - a_\mu)\chi_i + m_i \bar{\chi}_i \chi_i \\ &+ \frac{1}{4\pi}(\beta d\beta - 2\gamma d\beta - \beta_2 d\beta_2 + 2(A_c + \gamma - a)d\beta_2) \\ &- \frac{1}{4\pi}\alpha_1 d\alpha_1 - \frac{1}{4\pi}\alpha_2 d\alpha_2 + \frac{1}{2\pi}\left(\frac{1}{2}A_s + a\right)d\alpha_1 \\ &+ \frac{1}{2\pi}\left(-\frac{1}{2}A_s + a\right)d\alpha_2, \end{aligned} \tag{26}$$

where η_μ's are Pauli matrices acting on the Dirac spinor indices and we ignored the Maxwell terms for $A_c + \gamma - a$ coupled to the Dirac fermions. At the critical point, the χ_i's are gapless ($m_i = 0$). The masses $m_1 = m_2$ are enforced by the projective translation symmetry of the fermions. Properly integrating out χ_i when the masses are nonzero and χ_i filling a band with Chern number ± 1, requires a dual field β_1 and gives $\frac{\mp 1}{4\pi}\beta_1 d\beta_1 + \frac{1}{2\pi}\beta_1 d(A_c + \gamma - a)$, respectively.

When $m_1 = m_2 > 0$, ψ_1 fills a band with $C_1 = 1$ and the theory describes a $d + id$ superconductor. Integrating out fields like a, χ_i, γ gives an action (Appendix F)

$$\begin{aligned}\mathcal{L}_{d+id} &= \frac{1}{4\pi}(-2\alpha_c d\alpha_c + 4\beta_2 d\alpha_c - 2\beta_2 d\beta_2 + 2A_c d\alpha_c) \\ &- \frac{2}{4\pi}\alpha_s d\alpha_s + \frac{1}{2\pi}A_s d\alpha_s, \end{aligned} \tag{27}$$

with $\alpha_{c,s}$ related to $\alpha_{1,2}$ as in Sec. IV. If one identifies $\tilde{\beta} = \beta_2 - \alpha_c$, the action is identical to the $d + id$ superconductor action in Eq. (25).

When $m_1 = m_2 < 0$, ψ_1 fills a band with $C_1 = -1$ and the theory describes a CSL1. Integrating out χ_i and γ, β_2 gives an action as Eq. (6) (Appendix F), describing the response of CSL1 with the charge mode gapped.

B. Universal properties of the critical point

To obtain the transport properties of the critical theory, one integrates out α_c ($\alpha_{c,s}$ as defined in Sec. IV) in the critical action (26), writing $\Gamma = \gamma - a$, and the critical theory reads

$$\begin{aligned}\mathcal{L}_{\rm cri} &= \sum_{i=1,2} \bar{\chi}_i [\eta_\mu (i\partial_\mu + A_{c,\mu} + \Gamma_\mu)]\chi_i \\ &- \frac{1}{4\pi}\Gamma d\Gamma + \frac{2}{4\pi}A_c d\Gamma + \frac{1}{4\pi}A_c dA_c \\ &- \frac{2}{4\pi}\alpha_s d\alpha_s + \frac{1}{2\pi}A_s d\alpha_s. \end{aligned} \tag{28}$$

The physical currents $J = \delta L_{\rm cri}/\delta A_c$ are

$$\begin{aligned} 2\pi J_x &= 2\pi \mathcal{J}_x - E_y - e_y, \\ 2\pi J_y &= 2\pi \mathcal{J}_y + E_x + e_x, \end{aligned} \tag{29}$$

where we denote $\epsilon^{\mu\nu\rho}\partial_\nu A_{c,\rho} = (B, -E_y, E_x)$. In addition, we have $\epsilon^{\mu\nu\rho}\partial_\nu \Gamma_\rho = (b, -e_y, e_x)$ and $\mathcal{J}_\nu$ as the current for χ. The equations of motion for Γ are

$$\begin{aligned} 2\pi \mathcal{J}_x + e_y - E_y &= 0, \\ 2\pi \mathcal{J}_y - e_x + E_x &= 0. \end{aligned} \tag{30}$$

Combining the above relations and the assumed universal conductivity for χ at the critical point (QED-3), $\mathcal{J}_\nu = \sigma_\chi(E_\nu + e_\nu)$, one gets the conductivity from Eq. (29) as

$$2\pi\sigma_c = \begin{pmatrix} \frac{4\tilde{\sigma}_\chi}{\tilde{\sigma}_\chi^2+1} & \frac{-2(1-\tilde{\sigma}_\chi^2)}{\tilde{\sigma}_\chi^2+1} \\ \frac{2(1-\tilde{\sigma}_\chi^2)}{\tilde{\sigma}_\chi^2+1} & \frac{4\tilde{\sigma}_\chi}{\tilde{\sigma}_\chi^2+1} \end{pmatrix}, \tag{31}$$

where $\tilde{\sigma}_\chi = 2\pi\sigma_\chi$.

In summary, the deconfined superconductor-insulator critical point should have a nonzero universal conductivity shown in Eq. (31). Given that both the superconductor and the CSL insulator have zero Hall conductivity, a nonzero Hall effect only at the critical point is quite remarkable. There is also a spin quantum Hall effect $\frac{1}{8\pi}A_s dA_s$, which remains constant across the transition.

VI. CONCLUSIONS AND OUTLOOK

In summary, we propose two different phases from doping a $U(1)_2$ chiral spin liquid on triangular lattice. One possibility is a chiral metal from simple slave boson condensation picture. Another more exotic possibility is a topological superconductor obtained by putting both the slave boson and the spinon in a quantum Hall phase. We argue that these two scenarios are consistent with two recent numerical studies of doped CSL in two different parameter regimes. Our theory may be relevant to transition metal dichalcogenide heterobilayer where a spin 1/2 Hubbard model can be simulated on a triangular Moiré superlattice [70–73]. It has also been proposed that a generalized CSL with different topological order is possible in a $SU(4)$ model on Moiré bilayer [44]. In future it is interesting to extend our theory of doped CSL to the case with $SU(N)$ spin.

From a quantum criticality perspective, we propose an unconventional superconductor to Mott insulator transition, as described by a plateau transition of the charged holons. If we start from a $d + id$ superconductor, there are two different Mott transitions towards two different chiral spin liquid insulators. We also find a deconfined critical point between a translation symmetry breaking Chern insulator and a translation invariant topological superconductor. We hope to study this kind of deconfined critical points in more detail in the future.

ACKNOWLEDGMENTS

We thank E. Altman, O. Motrunich, and Z. Zhu for useful discussions. We acknowledge funding from a Simons Investigator award (A.V.) and the Simons Collaboration on Ultra-Quantum Matter, which is a grant from the Simons Foundation (No. 651440, A.V.). This research is funded in part by the Gordon and Betty Moore Foundation's EPiQS Initiative, Grant No. GBMF8683 to A.V.

APPENDIX A: $SU(2)$ AND $U(1)$ SLAVE BOSON FORMALISM

We remark that a full treatment of the parton representation for electrons have an $SU(2)$ gauge symmetry, which is given by two species of spin-0 holons $h_i = (b_{1,i}, b_{2,i})^T$ and spinons

$\psi_i = (\psi_{i,\uparrow}, \psi^\dagger_{i,\downarrow})^T$ to write the electron operators as

$$c_{i,\uparrow} = \frac{1}{\sqrt{2}} h_i^\dagger \psi_i = \frac{1}{\sqrt{2}} (b^\dagger_{1,i} f_{i,\uparrow} + b^\dagger_{2,i} f^\dagger_{i,\downarrow}),$$
$$c_{i,\downarrow} = \frac{1}{\sqrt{2}} h_i^\dagger (i\tau^y \psi_i^*) = \frac{1}{\sqrt{2}} (b^\dagger_{1,i} f_{i,\downarrow} - b^\dagger_{2,i} f^\dagger_{i,\uparrow}), \quad \text{(A1)}$$

where both ψ_i and $\bar{\psi}_i = i\tau^y \psi_i^*$ transform as doublets for $SU(2)$ group: $\psi_i \to U\psi_i$, $(U \in SU(2))$ and $\bar{\psi}_i \to U\bar{\psi}_i$, $(U \in SU(2))$. The physical electrons stay invariant under such $SU(2)$ transform given the holon doublet transform accordingly as $h_i \to U h_i$. The gauge-invariant condition for physical Hilbert space (excluding double occupancy) constrain each site to contain an $SU(2)$ singlet, i.e.,

$$h_i^\dagger \tau h_i + \psi_i^\dagger \tau \psi_i |\Psi_{\text{phys}}\rangle = 0, \quad \text{(A2)}$$

which for the τ^z component reads

$$b^\dagger_{1,i} b_{1,i} - b^\dagger_{2,i} b_{2,i} + \sum_s f^\dagger_{i,s} f_{i,s} = 1. \quad \text{(A3)}$$

In the main text parton construction, we effectively fix the gauge for the holon sector as $b_{i,2} = 0$ identically and leave out one holon $b_{i,1}$ as b in the main text. This is justified since given the $SU(2)$ gauge group, one could rotate a state to one with $b_{i,2} = 0$ without changing the physical state. The price is a reduced gauge group $U(1)$ away from half-filling, and that upon transforming the mean field for spinons with $SU(2)$ rotations, the state changes physically upon doping. For instance, in Eq. (8) one transforms the spinon ansatz from a $U(1)_2$ CSL1 to $d + id$ (CSL2), equivalent at half-filling, and yet upon doping holes, the state becomes a chiral metal and $d + id$ superconductor after condensing b_1, respectively. Conversely, one could fix the gauge for spinons and then different boson condensation leads to different physical states. In this paper we adopt the first approach, allowing only b_1 to condense, and hence different spinon ansatz, equivalent at half-filling, give different physical states upon doping. Therefore at $\theta = 0$ on triangular lattice CSLs, upon doping, either a $d + id$ or a chiral metal could emerge upon condensing different holon states. This is also true on square lattices (see Appendix C), where a $d + id$ ansatz with zero diagonal hopping is equivalent to a chiral spin liquid (DSL with a chiral mass) through an $SU(2)$ transform. Hence on square lattice doping a CSL gives either $d + id$ superconductor or a chiral metal.

APPENDIX B: COMPETING TRANSLATION BREAKING PAIRING STATE ON DOPING CSL1

At noted in the main text, at $\theta = 0$, the $U(1)_2$ CSL1 is equivalent to a projected $d + id$ spin liquid on triangular lattice. Hence upon doping the $U(1)_2$ CSL1 at $\theta = 0$, the resulting states are a competition between $d + id$ and chiral metal in Sec. III. When θ shifts from zero, however, one could still perform the gauge transform Eq. (8) on $U(1)_2$ CSL1 towards a $d + id$ pairing ansatz, which could be the competing pairing state with chiral metal upon doping the CSL1. Next we analyze the ansatz for such pairing state.

The CSL1 ansatz Eq. (3) becomes $\tilde{u}_{ij} = g_j^\dagger u_{i,j} g_i$ after the transform

$$\tilde{u}_{r,r+\hat{x}} = \frac{1}{\sqrt{3}} \begin{pmatrix} e^{i\theta} & \sqrt{2}e^{-i\theta} \\ \sqrt{2}e^{i\theta} & -e^{-i\theta} \end{pmatrix}, \quad (r_x \mod 2 = 0),$$
$$\tilde{u}_{r,r+\hat{x}} = \frac{1}{\sqrt{3}} \begin{pmatrix} e^{i\theta} & \sqrt{2}e^{i\theta} \\ \sqrt{2}e^{-i\theta} & -e^{-i\theta} \end{pmatrix}, \quad (r_x \mod 2 = 1),$$
$$\tilde{u}_{r,r+\hat{y}} = \frac{1}{\sqrt{3}} \begin{pmatrix} e^{i\theta} & \sqrt{2}e^{-i\theta - i\frac{2\pi}{3}} \\ \sqrt{2}e^{i\theta + i\frac{2\pi}{3}} & -e^{-i\theta} \end{pmatrix}, \quad (r_x \mod 2 = 0),$$
$$\tilde{u}_{r,r+\hat{y}} = \frac{1}{3} \begin{pmatrix} -i\left(e^{i\theta} + 2e^{-i\theta + i\frac{2\pi}{3}}\right) & \sqrt{2}i\left(e^{-i\theta + i\frac{2\pi}{3}} - e^{i\theta}\right) \\ \sqrt{2}i\left(-e^{i\theta - i\frac{2\pi}{3}} + e^{-i\theta}\right) & -i\left(e^{-i\theta} - 2e^{i\theta - i\frac{2\pi}{3}}\right) \end{pmatrix}, \quad (r_x \mod 2 = 1),$$
$$\tilde{u}_{r,r+\hat{y}+\hat{x}} = \frac{1}{\sqrt{3}} \begin{pmatrix} e^{-i\theta} & \sqrt{2}e^{i\theta + i\frac{2\pi}{3}} \\ \sqrt{2}e^{-i\theta - i\frac{2\pi}{3}} & -e^{i\theta} \end{pmatrix}, \quad (r_x \mod 2 = 0),$$
$$\tilde{u}_{r,r+\hat{y}+\hat{x}} = \frac{1}{3} \begin{pmatrix} i\left(e^{-i\theta} + 2e^{i\theta - i\frac{2\pi}{3}}\right) & \sqrt{2}i\left(-e^{i\theta - i\frac{2\pi}{3}} + e^{-i\theta}\right) \\ \sqrt{2}i\left(e^{-i\theta + i\frac{2\pi}{3}} - e^{i\theta}\right) & i\left(e^{i\theta} + 2e^{-i\theta + i\frac{2\pi}{3}}\right) \end{pmatrix}, \quad (r_x \mod 2 = 1). \quad \text{(B1)}$$

One sees that at $\theta = 0$, the above mean-field ansatz is identical to $d + id$ states in Eq. (7) at $\eta = \sqrt{2}\chi$, while $\theta \neq 0$, the pairing has $d + id$ symmetry yet the state breaks lattice translation, distinct from the conventional translation invariant $d + id$ states.

APPENDIX C: CHIRAL SPIN LIQUIDS ON SQUARE LATTICE

For a square lattice, under an appropriate gauge choice, the CSL mean-field ansatz in the spinor basis ψ reads

$$\begin{aligned} u_{r,r+\hat{x}} &= \cos(\theta)\tau^z + \sin(\theta)\tau^y, \\ u_{r,r+\hat{y}} &= \cos(\theta)\tau^z - \sin(\theta)\tau^y, \\ u_{r,r+\hat{x}+\hat{y}} &= \chi\cos(\theta)\tau^z + \eta\sin(\theta)\tau^x, \\ u_{r,r-\hat{x}+\hat{y}} &= \chi\cos(\theta)\tau^z - \eta\sin(\theta)\tau^x, (\chi, \eta \in R), \end{aligned} \quad \text{(C1)}$$

where the IGG is reduced to Z_2 when $\theta \neq n\pi/4$, $(n \in Z)$ and $\chi \neq 0$. This can be seen by calculating Wilson loop Φ around

a square or triangular loop on the square lattice,

$$\begin{aligned}\Phi_{\square} &= u_{r,r+\hat{x}}u_{r,r+\hat{y}}u_{r,r-\hat{x}}u_{r,r-\hat{y}},\\ &= \cos 4\theta - i\sin 4\theta\tau^x,\\ \Phi_{\triangle} &= u_{r,r+\hat{x}}u_{r,r+\hat{y}}u_{r,r-\hat{x}-\hat{y}} = \chi(\cos 2\theta\cos\theta\tau^z\\ &\quad + \sin 2\theta\cos\theta\tau^y) + \eta(\cos 2\theta\sin\theta\tau^x - i\sin 2\theta\sin\theta).\end{aligned} \tag{C2}$$

We note that the $d+id$ ansatz contain two different chiral spin liquids: (I) When $\theta = n\frac{\pi}{4}$ or $\chi = 0$ with arbitrary θ, the IGG is $U(1)$ and we get a CSL1 described by the $U(1)_2$ theory; (II) For a generic ansatz with diagonal hopping, the IGG is Z_2 and we have a CSL2 phase in the $\nu = 4$ of the Kitaev's 16-fold way.

We note that $d+id$ ansatz *contains* all square $U(1)$ DSL with a chiral mass states (CSL1). The ansatz for $U(1)$ CSL1 is a staggered flux one with diagonal hopping

$$\begin{aligned}u_{r,r+\hat{x}} &= \cos(\theta)\tau^z + i(-1)^{r_x+r_y}\sin(\theta)\tau^0,\\ u_{r,r+\hat{y}} &= \cos(\theta)\tau^z - i(-1)^{r_x+r_y}\sin(\theta)\tau^0,\\ u_{r,r+\hat{x}+\hat{y}} &= (-1)^{r_x+r_y}\eta\sin(\theta)\tau^z,\\ u_{r,r-\hat{x}+\hat{y}} &= -(-1)^{r_x+r_y}\eta\sin(\theta)\tau^z,\ (\eta\in R),\end{aligned} \tag{C3}$$

where IGG is $U(1)$ generated by τ^z. By a gauge transform, such an ansatz is equivalent to $d+id$ with $\chi = 0$ in Eq. (C1). The gauge transform reads

$$\psi_r \to \frac{1}{\sqrt{2}}(1 + (-1)^{r_x+r_y}i\tau^y)\psi_r. \tag{C4}$$

Hence a generic CSL1 phase on square lattice can be written in the $d+id$ ansatz. After doping a CSL1, we can get a translation invariant $d+id$ superconductor from the simple holon condensation picture, in contrast to a triangular lattice.

APPENDIX D: NUMERICAL PROCEDURE FOR BERRY CURVATURES AND DIRAC FERMIONS NEAR $\theta = \pi/6$

We present some numerical details for Berry curvatures and analytical derivation of Dirac Hamiltonian near $\theta = \pi/6$ gapless point.

Berry connections for Bloch wave functions $u(\mathbf{k})$ for the electrons can be approximated numerically as $A_\epsilon d\epsilon = \mathrm{Arg}\langle u(\mathbf{k}+\epsilon)|u(\mathbf{k})\rangle$ where ϵ is a small vector increment in momentum space and Arg gives the phase of the complex number. We mesh the $kx - ky$ plane with increments $\epsilon_1 = (\delta, 0)$, $\epsilon_2 = (0, \delta)$, where k_x, k_y are measured by the reciprocal vectors for basis vector $\hat{x}, \hat{y}$ in the main text, shown in Fig. 7(b) and δ at the order of 0.01 radian. The total Berry curvature on one elementary plaquette of the momentum mesh is given by [shown in Fig. 7(a)]

$$\begin{aligned}\mathcal{F}(\mathbf{k})d^2k &= \mathrm{Arg}\langle u(\mathbf{k}+\epsilon_1)|u(\mathbf{k})\rangle\\ &\quad + \mathrm{Arg}\langle u(\mathbf{k}+\epsilon_1+\epsilon_2)|u(\mathbf{k}+\epsilon_1)\rangle\\ &\quad + \mathrm{Arg}\langle u(\mathbf{k}+\epsilon_2)|u(\mathbf{k}+\epsilon_1+\epsilon_2)\rangle\\ &\quad + \mathrm{Arg}\langle u(\mathbf{k})|u(\mathbf{k}+\epsilon_2)\rangle.\end{aligned} \tag{D1}$$

Note that for bands with nonzero Chern number, Berry curvature on some plaquettes in k space may have discontinuity of $\pm 2\pi$, since total Berry curvature of one band in the above discretized formula is always zero. One manually makes up for the 2π discontinuities and then sum the Berry curvature totals $\mathcal{F}(\mathbf{k})d^2k$ over filled $\mathbf{k}$ states for Hall conductivity of the spinons.

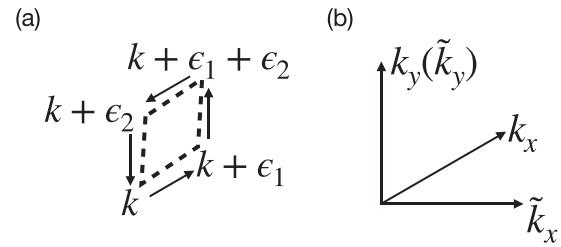

FIG. 7. (a) The numerical procedure to calculate Berry curvature of Bloch wave function in k space. One circles around an elementary plaquette (dashed diamond) and adds up the phase of overlap of wave functions at the ends of each bond. (b) The reciprocal vectors for $\hat{x}, \hat{y}$ lattice vectors used in main text and the orthogonal coordinates used for Dirac Hamiltonian Eq. (D3) $\tilde{k}_x, \tilde{k}_y$.

At θ close to $\pm\pi/6$, in the *spinon* Hamiltonian, Dirac cones with a small mass emerge near half-filling. We derive the Dirac Hamiltonian near the gapless point. The spinon Hamiltonian Eq. (3) in k space reads

$$\begin{aligned}\mathcal{H}_{\mathrm{spinon}} &= \sum_k \psi_k^\dagger(-2\cos(\theta+k_y)\tau^z\\ &\quad - 2\cos(\theta+k_x)\tau^x + 2\cos(\theta-k_x-k_y)\tau^y)\psi_k,\end{aligned} \tag{D2}$$

where $\psi_k = (f_{\uparrow,k}, f^\dagger_{\downarrow,-k})^T$. The k space Hamiltonian can be Taylor expanded near the gapless point, e.g., $\theta = \pi/6$, $(k_x, k_y) = (\pi/3, \pi/3)$ and we transform to orthogonal momentum coordinates shown in Fig. 7(b) $\tilde{k}_x = \frac{\sqrt{3}}{2}k_x$, $\tilde{k}_y = k_y + k_x/2$,

$$\begin{aligned}\mathcal{H}_{\mathrm{Dirac}} &= 2\left[\left(\frac{2}{\sqrt{3}}\tau^x - \frac{1}{\sqrt{3}}\tau^z - \frac{1}{\sqrt{3}}\tau^y\right)\tilde{k}_x + (\tau^z - \tau^y)\tilde{k}_y\right.\\ &\quad \left. + \left(\theta - \frac{\pi}{6}\right)(\tau^z + \tau^x + \tau^y)\right],\end{aligned} \tag{D3}$$

with the matrices multiplying $\tilde{k}_x, \tilde{k}_y, \sqrt{\frac{3}{2}}(\theta - \pi/6)$ obeying the anticommutation relations of gamma matrices for the Dirac Hamiltonian in $(2+1)D$ up to an overall factor $2\sqrt{2}$. Hence indeed the band can be approximated by a Dirac fermion with a small mass. Another Dirac cone appears at $(\pi/3, -2\pi/3)$ in k-space with the same chirality. Note the velocity is uniform, $v = 2\sqrt{2}$ and the mass $m = 2\sqrt{3}(\theta - \pi/6)$. The Berry curvature of the two-component spinor system has been well studied: representing the components of the Dirac Hamiltonian $H_{\mathrm{Dirac}} = vk_x\gamma^1 + vk_y\gamma^2 + m\gamma^0$ in a unit vector $\hat{n}(\mathbf{k}) = \frac{(vk_x, vk_y, m)}{\sqrt{v^2(k_x^2+k_y^2)+m^2}}$, the Berry curvature reads

$$\mathcal{F}(\mathbf{k}) = \frac{\hat{n}\cdot d_{k_x}\hat{n}\times d_{k_y}\hat{n}}{2}. \tag{D4}$$

Pictorially the Berry phase accumulated is given by $1/2$ times the solid angle that $\hat{n}(\mathbf{k})$ sweeps through during an adiabatic process.

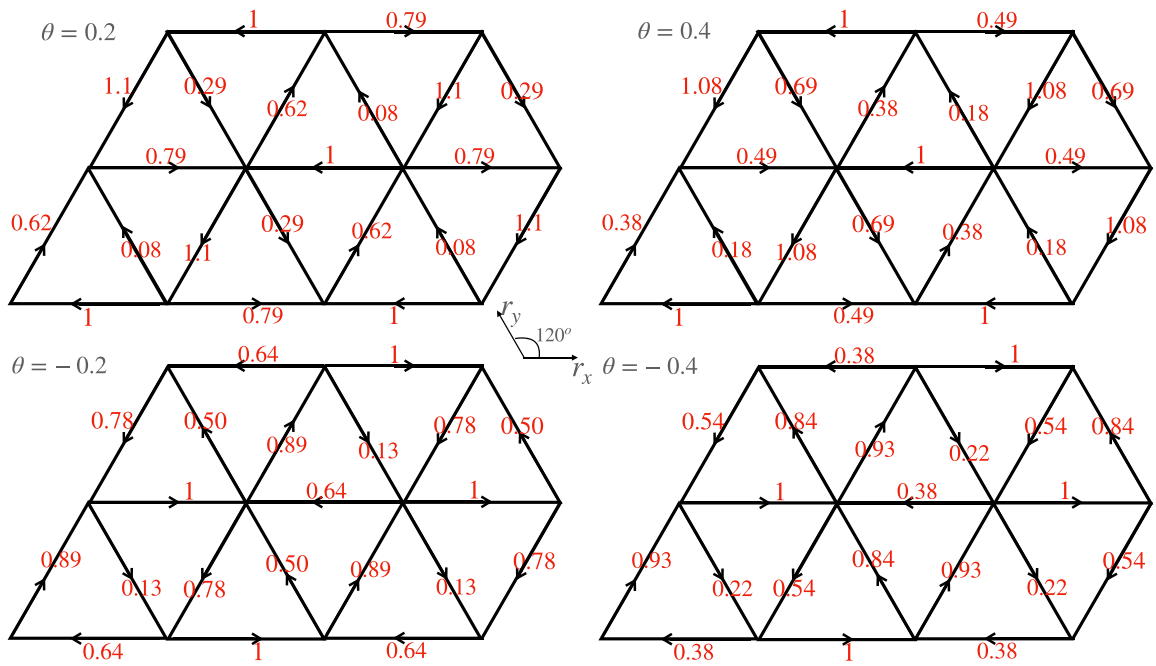

FIG. 8. The relative current strength $I_{\text{bond}\langle ij\rangle} = \text{Im}[c_i^\dagger c_j]$ of the chiral metal upon infinitesimal doping of holes shown as red numbers on the bond (θ as shown in upper left of each panel) with arrows indicating current directions. We assume the holons condense fully at Γ. The currents for infinitesimal electron doping are negative of those in hole doped case, and with a shift of the y direction bonds.

To express the Hall conductivity as one varies electron doping x, one first obtains the density of states near the Dirac cone as

$$\rho(E) = \frac{dN}{dE} = \frac{2\pi k dk}{v dk \frac{4\pi^2 \sin\frac{\pi}{3}}{L_x L_y}}, \tag{D5}$$

where we used the area a state occupied in k space for a triangular system with size L_x, L_y as $\frac{4\pi^2 \sin\frac{\pi}{3}}{L_x L_y}$ and k as the norm of $\mathbf{k}$ since the dispersion is uniform around Dirac cones. At doping level of x, the states in a circle around Dirac point with radius k_c in valence band are emptied, k_c given by

$$\int_0^{k_c} dE\,\rho(E) = L_x L_y \frac{x}{4},$$
$$k_c^2 = \pi x \sin\frac{\pi}{3}, \tag{D6}$$

where the factor $1/4$ comes from the 4 Dirac cones in 2 spinon conduction bands.

The Berry curvature accumulated from states in a circle of radius k_c is given by the solid angle swept by $\hat{n}$ from $|k| = 0$, $\hat{n} = (0, 0, 1)$ to $|\mathbf{k}| = k_c$, $\hat{n}(\mathbf{k}) = \frac{(vk_x, vk_y, m)}{\sqrt{v^2k_c^2+m^2}}$, hence

$$\int_{|k|<k_c} d^2k\mathcal{F}(\mathbf{k}) = \frac{2\pi}{2}\left(1 - \frac{m}{\sqrt{m^2 + v^2k_c^2}}\right), \tag{D7}$$

substituting k_c from Eq. (D6) and m, v from previous analysis, one gets the Hall conductivity as the total Chern number from two spinon valence bands $C = 2$, minus the contributions from states around Dirac cones as

$$\sigma_{xy} = \frac{2e^2}{h} - \frac{4\pi e^2}{4\pi^2\hbar}\left(1 - \frac{2\sqrt{3}\Delta}{\sqrt{12\Delta^2 + 4\sqrt{3}\pi x}}\right), \tag{D8}$$

where $\Delta = |\pi/6 - \theta|$, which is the expression for σ_{xy} as in Eq. (17).

APPENDIX E: CALCULATION OF SPECTRAL FUNCTION $A(k, \omega = 0^+)$

We define a plane-wave basis for electrons as

$$c_k^\dagger = \frac{1}{L}\sum_r e^{ik\cdot r} c_i^\dagger,$$
$$c_{k,A}^\dagger = \frac{1}{L}\sum_{r\in A} e^{ik\cdot r} c_i^\dagger, \tag{E1}$$
$$c_{k,B}^\dagger = \frac{1}{L}\sum_{r\in B} e^{ik\cdot r} c_i^\dagger.$$

The first one is used in defining the spectral function as one measures in ARPES. The latter two correspond to plane waves on sublattices A, B, respectively. Taking the origin at A site, these operators have the relation

$$c_k^\dagger = c_{k,A}^\dagger + c_{k,B}^\dagger,$$
$$c_k^\dagger = c_{k+\mathbf{G}_1,A}^\dagger - c_{k+\mathbf{G}_1,B}^\dagger, \tag{E2}$$

where we used $e^{i\mathbf{G}_1\cdot r_{AB}} = -1$, where r_{AB} is the vector connecting sites on two sublattices.

The spectral function measured in the ground state at frequency $\omega = 0^+$ is contributed by eigenstates $u_k^\dagger = \alpha_k c_{k,A}^\dagger + \beta_k c_{k,B}^\dagger$ on the Fermi pockets. The coefficients are related to those of the spinon eigenstates by holon condensed

values, i.e.,

$$\alpha_k = \sum_{k'} u_{b,k'}(A)\alpha_{k-k',f},$$
$$\beta_k = \sum_{k'} u_{b,k'}(B)\beta_{k-k',f}, \tag{E3}$$

where $\alpha_{k,f}, \beta_{k,f}$ are the coefficients for sublattice A, B wave functions for spinon eigenstates and $u_{b,k}(A, B)$ are the holon condensation $\langle b\rangle$ in reciprocal space as discussed in Eq. (11), nonvanishing only for $k = \Gamma, M_2(M_2 = (0, \pi))$. Note that spinon states at $k, k + M_2$ have the same energy due to the projective symmetry T_x with a momentum boost of M_2.

This overlap of the plane wave basis for electrons reads

$$\langle u_{k'}|c_k^\dagger|0\rangle = \delta_{k,k'}(\alpha_k + \beta_k) + \delta_{k,k'\pm\mathbf{G}_1}(\alpha_{k'} - \beta_{k'}). \tag{E4}$$

The spectral function is given by

$$A(\mathbf{k}, \omega = 0^+) = 2\pi \int_{k'\in FS} dk' |\langle u_{k'}|c_k^\dagger|0\rangle|^2. \tag{E5}$$

Since the original BZ measured in ARPES is double the size of the reduced one, when measured momenta k lie outside of the reduced BZ, one effectively excites states inside the reduced BZ at its equivalent momentum (i.e., obtained by a translation of a reciprocal lattice vector $\mathbf{G}_1$).

Using (E4) to express the spectral function, one finds a simple expression

$$A(\mathbf{k}, \omega = 0^+) = \begin{cases} 2\pi|\alpha_k + \beta_k|^2 & \mathbf{k} \in \text{reduced BZ} \\ 2\pi|\alpha_{ko} - \beta_{ko}|^2 & \mathbf{ko} = \mathbf{k} \pm \mathbf{G}_1 \in \text{reduced BZ}, \end{cases} \tag{E6}$$

where **ko** is the equivalent momenta for **k** in the reduced BZ.

APPENDIX F: A CONCRETE MEAN FIELD THEORY OF THE TOPOLOGICAL SUPERCONDUCTOR AND DECONFINED TRANSITION

Here we try to construct a concrete mean-field theory of the topological superconductor and writing down a mean- field ansatz for it.

To simplify the construction of the bIQHE state, we introduce two slave bosons, each of which has filling 1/2 per site. We will hybridize them in the last stage so the final theory should be smoothly connect to that of one slave boson. For the discussion of Mott transition at fixed density $n_c = 1$, we use $U(1)$ slave boson theory, instead of the $SU(2)$ version. The cost is that we cannot keep track of the C_6 symmetry. But we can still keep track of translations T_x, T_y. We will show explicitly that our proposed ansatz is invariant under T_x and T_y.

The modified slave boson theory is

$$c_{i;\uparrow} = b_i f_{i;\uparrow}, \tag{F1}$$

$$c_{i;\downarrow} = \tilde{b}_i f_{i;\downarrow}. \tag{F2}$$

This will introduce two independent $U(1)$ gauge fields: a and $\tilde{a}$. But we will lock them together with a Higgs term $b_i^\dagger \tilde{b}_i +$ h.c.. Note the above parton construction does not satisfy the $SU(2)$ spin rotation symmetry. We can only keep track of the S_z quantum number. As a result, the state constructed in this way may break the $SU(2)$ spin rotation down to $U(1)$.

Now the constraint is that

$$n_{i;b} = n_{i;f_\uparrow},$$
$$n_{i;\tilde{b}} = n_{i;f_\downarrow}. \tag{F3}$$

So on average we have $n_b = n_{\tilde{b}} = \frac{1}{2}$ per site. To describe the bIQHE phase, we do a further fractionalization:

$$b_i = d_i \psi_{i;1},$$
$$\tilde{b}_i = \tilde{d}_i \psi_{i;2}, \tag{F4}$$

which introduces another two $U(1)$ gauge field $\gamma, \tilde{\gamma}$.

In total, the electron is fractionalized in the following way:

$$c_{i;\uparrow} = d_i \psi_{i;1} f_{i;\uparrow},$$
$$c_{i;\downarrow} = \tilde{d}_i \psi_{i;2} f_{i;\downarrow}. \tag{F5}$$

We assign the charge in the following way: ψ_1 couples to $-a + A_c + \gamma$, ψ_2 couples to $-\tilde{a} + A_c + \tilde{\gamma}$, d couples to $-\gamma$, $\tilde{d}$ couples to $-\tilde{\gamma}$, $f_\uparrow$ couples to $\frac{1}{2}A_s + a$, and $f_\downarrow$ couples to $-\frac{1}{2}A_s + \tilde{a}$.

We consider the following mean-field ansatz:

$$H = H_f + H_d + H_{\psi_1} + H_{\psi_2} - \lambda \sum_i (\psi_{i;1}^\dagger \psi_{i;2} + \text{h.c.}). \tag{F6}$$

First, H_f is just the mean-field ansatz of the fermionic spinons. $d, \tilde{d}$ hybridize together and have a mean-field ansatz with 0 flux per unit cell ($T_x T_y = T_y T_x$.). Their hybridization locks $\gamma = \tilde{\gamma}$, so we will only keep γ in the following analysis. We want the PSG of d to be completely trivial. The nontrivial PSG of b is inherited completely by ψ. Because there are two orbitals formed by $d, \tilde{d}$, there can be a Chern insulator with $C_d = 1$ even if the ansatz does not break translation symmetry. We show a generic mean field for $d, \tilde{d}$ with such properties:

$$\begin{aligned} H_d = &\sum_{\langle ij\rangle} [d_i^\dagger d_j - \tilde{d}_i^\dagger \tilde{d}_j] + \sum_r p_1 d_r^\dagger \big(\tilde{d}_{r+\hat{x}} + e^{i\frac{2\pi}{3}} \tilde{d}_{r+\hat{y}} \\ &+ e^{-i\frac{2\pi}{3}} \tilde{d}_{r-\hat{x}-\hat{y}}\big) + \sum_r p_2 d_r^\dagger \big(\tilde{d}_{r-\hat{x}} + e^{i\frac{2\pi}{3}} \tilde{d}_{r-\hat{y}} \\ &+ e^{-i\frac{2\pi}{3}} \tilde{d}_{r+\hat{x}+\hat{y}}\big) + \text{h.c.}, \end{aligned} \tag{F7}$$

which preserves translation and the mixed hopping between $d, \tilde{d}$ has angular momentum 2. This mean-field dispersion is generically gapped except with particular parameters, e.g., $p_1 p_2 = 0$ and may have a nonvanishing Chern number, e.g., when $p_1 = p_2 = 1 + i$, the valence band has a Chern number $C_d = 1$.

ψ_1 and ψ_2 have mean-field ansatz with $T_x T_y = -T_y T_x$, which should be similar to that of spinon f introduced in the main text. They have a Chern number $C_1 = \pm 1$ and $C_2 = 1$. The mean field we use for ψ is those for the CSL1 in Eq. (3) with $\theta = \pi/6 \pm \delta$, ($\delta > 0$) for Chern number $C = \mp 1$, respectively.

In the following we analyze the cases with $\lambda = 0$ and $\lambda \neq 0$ separately. The topological superconductor discussed in the main text corresponds to $\lambda \neq 0$.

1. $\lambda = 0$: $p + ip$ superconductor

We deal with the special case of $\lambda = 0$ first. In this case, we need to deal with two $U(1)$ gauge field a and $\tilde{a}$, which couples to $f_\uparrow$, b and $f_\downarrow$, $\tilde{b}$, respectively. First, integration of the spinon f_σ gives

$$L_f = -\frac{1}{4\pi}\alpha_1 d\alpha_1 - \frac{1}{4\pi}\alpha_2 d\alpha_2 + \frac{1}{2\pi}\left(\frac{1}{2}A_s + a\right)d\alpha_1 + \frac{1}{2\pi}\left(-\frac{1}{2}A_s + \tilde{a}\right)d\alpha_2, \tag{F8}$$

where α_1, α_2 are introduced to describe the IQHE of the fermionic spinons.

Next we consider the ansatz with $C_d = -1, C_1 = C_2 = 1$. The slave boson part has the action

$$L_b = \frac{1}{4\pi}\beta d\beta - \frac{1}{2\pi}\gamma d\beta - \frac{1}{4\pi}\beta_1 d\beta_1 - \frac{1}{4\pi}\beta_2 d\beta_2 + \frac{1}{2\pi}(A_c + \gamma - a)d\beta_1 + \frac{1}{2\pi}(A_c + \gamma - \tilde{a})d\beta_2. \tag{F9}$$

Integration of γ locks $\beta = \beta_1 + \beta_2$, then

$$L_b = \frac{1}{4\pi}\beta_1 d\beta_2 + \frac{1}{4\pi}\beta_2 d\beta_1 + \frac{1}{2\pi}(A_c - a)d\beta_1 + \frac{1}{2\pi}(A_c - \tilde{a})d\beta_2. \tag{F10}$$

The final action is $L_c = L_b + L_f$. By integrating a and $\tilde{a}$, we can lock $\beta_1 = \alpha_1$ and $\beta_2 = \alpha_2$. We can then reach the final action:

$$L_c = -\frac{1}{4\pi}\alpha_1 d\alpha_1 - \frac{1}{4\pi}\alpha_2 d\alpha_2 + \frac{1}{4\pi}\alpha_1 d\alpha_2 + \frac{1}{4\pi}\alpha_2 d\alpha_1 + \frac{1}{2\pi}\left(A_c + \frac{1}{2}A_s\right)d\alpha_1 + \frac{1}{2\pi}\left(A_c - \frac{1}{2}A_s\right)d\alpha_2. \tag{F11}$$

By relabeling $\alpha_1 = \alpha_c + \alpha_s$ and $\alpha_2 = \alpha_c - \alpha_s$, we get

$$L_c = \frac{2}{2\pi}A_c d\alpha_c - \frac{4}{4\pi}\alpha_s d\alpha_s + \frac{1}{2\pi}A_s d\alpha_s. \tag{F12}$$

The above action is equivalent to the theory of $p + ip$ superconductor, which is in the $\nu = 2$ class of Kitaev's 16-fold way classification [61]. $p + ip$ pairing is possible in the spin-triplet channel of $c_\uparrow c_\downarrow$. This is also an indication that the full $SU(2)$ spin rotation symmetry is broken in this state.

2. $\lambda \neq 0$: $d + id$ superconductor

We will show that the case with $\lambda \neq 0$ gives a superconductor with the same topological property as the spin singlet $d + id$ superconductor.

With $\lambda \neq 0$, the term $-\lambda\psi^\dagger_{i;1}\psi_{i;2} + \text{h.c.}$ locks $a = \tilde{a}$ (Note that we already lock $\gamma = \tilde{\gamma}$ by the hybridization between d and $\tilde{d}$.). After that, the action for the slave boson part should be modified as

$$L_b = \frac{1}{4\pi}\beta_1 d\beta_2 + \frac{1}{4\pi}\beta_2 d\beta_1 + \frac{1}{2\pi}(A_c - a)d\beta_1 + \frac{1}{2\pi}(A_c - a)d\beta_2, \tag{F13}$$

which is exactly the action in Eq. (19) of the main text.

L_f is also modified to

$$L_f = -\frac{1}{4\pi}\alpha_1 d\alpha_1 - \frac{1}{4\pi}\alpha_2 d\alpha_2 + \frac{1}{2\pi}\left(\frac{1}{2}A_s + a\right)d\alpha_1 + \frac{1}{2\pi}\left(-\frac{1}{2}A_s + a\right)d\alpha_2, \tag{F14}$$

which is the same as Eq. (18) in the main text.

Then the analysis in the main text shows that this state is topologically equivalent to $d + id$ superconductor. Finally, let us comment on the spin rotation symmetry. Our formalization only explicitly preserve $U(1)$ spin rotation corresponding to S_z because we have two different slave bosons $b, \tilde{b}$ for the two spins. When $\lambda = 0$, there are two $U(1)$ gauge fields $a, \tilde{a}$. This strongly breaks spin rotation symmetry, and thus we get a state consistent with a spin-triplet $p + ip$ superconductor. When we increase λ, we couple b_i and $\tilde{b}_i$ together. In the limit that this hybridization is very large, we can keep only one $b'_i = \frac{1}{\sqrt{2}}(b_i + \tilde{b}_i)$ and then we recover the usual slave boson theory, which explicitly preserves the $SU(2)$ spin rotation. Therefore, we believe the phase constructed in this section can smoothly crossover to the spin-singlet $d + id$ superconductor when we increase the hybridization λ.

3. Model wave function

A wave function can be written down based on the above parton construction:

$$\Psi(\mathbf{x}_1, \cdots \mathbf{x}_N) = P_G \Psi_{d,\tilde{d}}(\mathbf{x}_1, \cdots \mathbf{x}_N)\Psi_\psi(\mathbf{x}_1, \cdots \mathbf{x}_N)\Psi_f(\mathbf{x}_1, \cdots \mathbf{x}_N), \tag{F15}$$

where P_G is the projection to enforce the constraints in Eq. (F5) and $\Psi_{d,\tilde{d}}, \Psi_\psi, \Psi_f$ are the ground state wave functions of the mean field discussed in Eq. (F6).

4. Deconfined CSL to superconductor transition

The critical point is described by changing C_1 from -1 to 1. This is captured by mass changing of two Dirac cones $\chi_{1,2}$ with momenta $(\pi/3, \pi/3)$, $(\pi//3, -2\pi/3)$, obtained by the changing of θ in ψ_1 mean-field Eq. (3) from $\pi/6 + \delta$ to $\pi/6 - \delta$, $(\delta > 0)$. Because ψ_1 satisfies the projective translation symmetry $T_x T_y = -T_y T_x$, the mass of the two Dirac cones $\chi_{1,2}$ at $\theta = \pi/6$ are guaranteed to be the same by the translation symmetry. The translation acts projectively on two Dirac cones as

$$T_x : (\chi_1, \chi_2)^T \to e^{-i\frac{\pi}{3}}(\eta^x\chi_2, \eta^x\chi_1)^T,$$
$$T_y : (\chi_1, \chi_2)^T \to \text{diag}\left(e^{-i\frac{\pi}{3}}, -e^{-i\frac{\pi}{3}}\right)(\chi_1, \chi_2)^T, \tag{F16}$$

where η^x is the Pauli matrix on the Dirac indices of the Dirac fermions.

Adding up the Dirac fermions and actions for $\psi_2, d, \tilde{d}, f$, etc., one has for the critical action,(identifying $\gamma = \tilde{\gamma}, a = \tilde{a}$)

$$\mathcal{L}_{\text{cri}} = \sum_{i=1,2}\bar{\chi}_i\eta_\mu(i\partial_\mu - a_\mu + A_{c,\mu} + \gamma_\mu)\chi_i + m_i\bar{\chi}_i\chi_i + \frac{1}{4\pi}(\beta d\beta - 2\gamma d\beta - \beta_2 d\beta_2 + 2(A_c + \gamma - a)d\beta_2)$$

$$-\frac{1}{4\pi}\alpha_1 d\alpha_1 - \frac{1}{4\pi}\alpha_2 d\alpha_2 + \frac{1}{2\pi}\left(\frac{1}{2}A_s + a\right)d\alpha_1 + \frac{1}{2\pi}\left(-\frac{1}{2}A_s + a\right)d\alpha_2, \tag{F17}$$

where the first line describes critical theory for ψ_1 ($m = 0$ at critical point), the second line describes d, $\tilde{d}$, ψ_2, and the last line for the spinon action.

With nonzero masses ($m_1 = m_2$ by the projective translation symmetry), one integrates out χ. To be more precise, we should introduce another field β_1 for describing the state $C_1 = \pm 1$ after integrating out χ: $\frac{\mp 1}{4\pi}\beta_1 d\beta_1 + \frac{1}{2\pi}\beta_1 d(A_c + \gamma - a)$.

When $m_1 = m_2 > 0$, ψ_1 fills a band with $C_1 = 1$ and the theory should describe a $d + id$ superconductor. Rewriting $\gamma = \Gamma + a$, $\alpha_c = \frac{\alpha_1+\alpha_2}{2}$, $\alpha_s = \frac{\alpha_1-\alpha_2}{2}$ and integrating out a gives $\beta = 2\alpha_c$. The critical action becomes

$$\mathcal{L}_{\text{cri}} = \sum_{i=1,2} \bar{\chi}_i \eta_\mu (i\partial_\mu + A_{c,\mu} + \Gamma_\mu)\chi_i + m_i \bar{\chi}_i \chi_i + \frac{1}{4\pi}(2\alpha_c d\alpha_c - 4\Gamma d\alpha_c - \beta_2 d\beta_2 + 2(A_c + \Gamma)d\beta_2) - \frac{2}{4\pi}\alpha_s d\alpha_s + \frac{1}{2\pi}A_s d\alpha_s. \tag{F18}$$

Integrating out χ_i, Γ gives $2\alpha_c = \beta_1 + \beta_2$ and an action

$$\mathcal{L}_{d+id} = \frac{1}{4\pi}(-2\alpha_c d\alpha_c + 4\alpha_c d\beta_2 - 2\beta_2 d\beta_2 + 4A_c d\alpha_c) - \frac{2}{4\pi}\alpha_s d\alpha_s + \frac{1}{2\pi}A_s d\alpha_s. \tag{F19}$$

If one identifies $\tilde{\beta} = \alpha_c - \beta_2$ and rewriting the action in $\tilde{\beta}$, α_c, the action is identical to the $d + id$ superconductor action in Eq. (25) with gapless α_c mode coupled to A_c, hence superconducting.

When $m_1 = m_2 < 0$, ψ_1 fills a band with $C_1 = -1$ and the theory should describe a CSL1. Integrating out χ_i gives $\frac{1}{4\pi}\beta_1 d\beta_1 + \frac{1}{2\pi}\beta_1 d(A_c + \gamma - a)$, and integrating out γ in Eq. (F17) gives $\beta = -(\beta_1 + \beta_2)$ and an action

$$\mathcal{L}_{\text{CSL}} = \frac{1}{4\pi}[2\beta_1 d\beta_1 + 2\beta_1 d\beta_2 + 2(A_c - a)d(\beta_1 + \beta_2)] - \frac{1}{4\pi}\alpha_1 d\alpha_1 + \frac{1}{2\pi}\left(a + \frac{1}{2}A_s\right)d\alpha_1 - \frac{1}{4\pi}\alpha_2 d\alpha_2 + \frac{1}{2\pi}\left(a - \frac{1}{2}A_s\right)d\alpha_2. \tag{F20}$$

Integrating β_2 locks $\beta_1 = a - A_c$. Substituting it into the action, we find that the terms from the slave boson part cancel each other and we are left with the action from the fermionic spinon:

$$\mathcal{L}_{\text{CSL}} = -\frac{1}{4\pi}\alpha_1 d\alpha_1 + \frac{1}{2\pi}\left(a + \frac{1}{2}A_s\right)d\alpha_1 - \frac{1}{4\pi}\alpha_2 d\alpha_2 + \frac{1}{2\pi}\left(a - \frac{1}{2}A_s\right)d\alpha_2. \tag{F21}$$

Integrating a locks $\alpha_1 = -\alpha_2 = \alpha$, and we obtain the final action for the $U(1)_2$ CSL1:

$$\mathcal{L}_{\text{CSL}} = -\frac{2}{4\pi}\alpha d\alpha + \frac{1}{2\pi}A_s d\alpha. \tag{F22}$$

[1] P. W. Anderson, The resonating valence bond state in La_2CuO_4 and superconductivity, Science **235**, 1196 (1987).

[2] P. A. Lee, N. Nagaosa, and X.-G. Wen, Doping a Mott insulator: Physics of high-temperature superconductivity, Rev. Mod. Phys. **78**, 17 (2006).

[3] X. G. Wen, Symmetries of the superconducting order parameters in the doped spin-liquid state, Phys. Rev. B **41**, 4212 (1990).

[4] D. S. Rokhsar, Pairing in Doped Spin Liquids: Anyon Versus d-Wave Superconductivity, Phys. Rev. Lett. **70**, 493 (1993).

[5] M. Sigrist, T. M. Rice, and F. C. Zhang, Superconductivity in a quasi-one-dimensional spin liquid, Phys. Rev. B **49**, 12058 (1994).

[6] M. Fabrizio, Superconductivity from doping a spin-liquid insulator: A simple one-dimensional example, Phys. Rev. B **54**, 10054 (1996).

[7] T. Senthil and M. P. A. Fisher, Z_2 gauge theory of electron fractionalization in strongly correlated systems, Phys. Rev. B **62**, 7850 (2000).

[8] T. Senthil and P. A. Lee, Cuprates as doped U (1) spin liquids, Phys. Rev. B **71**, 174515 (2005).

[9] R. M. Konik, T. M. Rice, and A. M. Tsvelik, Doped Spin Liquid: Luttinger Sum Rule and Low Temperature Order, Phys. Rev. Lett. **96**, 086407 (2006).

[10] L. Balents and S. Sachdev, Dual vortex theory of doped Mott insulators, Ann. Phys. **322**, 2635 (2007).

[11] T. Watanabe, H. Yokoyama, Y. Tanaka, Jun-ichiro Inoue, and M. Ogata, Variational Monte Carlo studies of pairing symmetry for the t-J model on a triangular lattice, J. Phys. Soc. Jpn. **73**, 3404 (2004).

[12] G. Karakonstantakis, L. Liu, R. Thomale, and S. A. Kivelson, Correlations and renormalization of the electron-phonon coupling in the honeycomb Hubbard ladder and superconductivity in polyacene, Phys. Rev. B **88**, 224512 (2013).

[13] K. S. Chen, Z. Y. Meng, U. Yu, S. Yang, M. Jarrell, and J. Moreno, Unconventional superconductivity on the triangular lattice Hubbard model, Phys. Rev. B **88**, 041103(R) (2013).

[14] S. R. White, D. J. Scalapino, and S. A. Kivelson, One Hole in the Two-Leg t-J Ladder and Adiabatic Continuity to the Noninteracting Limit, Phys. Rev. Lett. **115**, 056401 (2015).

[15] J. Venderley and E. A. Kim, Density matrix renormalization study of superconductivity in the triangular lattice Hubbard Model, Phys. Rev. B **100**, 060506(R) (2019).

[16] K. Li, S.-L. Yu, and J.-X. Li, Global phase diagram, possible chiral spin liquid, and topological superconductivity in the triangular Kitaev-Heisenberg model, New J. Phys. **17**, 043032 (2015).

[17] Z. A. Kelly, M. J. Gallagher, and T. M. McQueen, Electron Doping a Kagome Spin Liquid, Phys. Rev. X **6**, 041007 (2016).

[18] B. Ye, A. Mesaros, and Y. Ran, Ferromagnetism and d+id superconductivity in 1/2 doped correlated systems on triangular lattice, arXiv:1604.08615 [cond-mat.str-el].

[19] Y.-F. Jiang, H. Yao, and F. Yang, Possible superconductivity with Bogoliubov Fermi surface in lightly doped Kagome U(1) spin liquid, arXiv:2003.02850.

[20] C. Peng, Y.-F. Jiang, T. P. Devereaux, and H.-C. Jiang, Evidence of pair-density wave in doping Kitaev spin liquid on the honeycomb lattice, arXiv:2008.03858.

[21] Y. Gannot, Y.-F. Jiang, and S. A. Kivelson, Hubbard ladders at small U revisited, Phys. Rev. B **102**, 115136 (2020).

[22] X.-G. Wen, Quantum order: A quantum entanglement of many particles, Phys. Lett. A **300**, 175 (2002).

[23] X.-G. Wen, Quantum orders and symmetric spin liquids, Phys. Rev. B **65**, 165113 (2002)

[24] T. Senthil, Theory of a continuous Mott transition in two dimensions, Phys. Rev. B **78**, 045109 (2008).

[25] V. Kalmeyer and R. B. Laughlin, Equivalence of the Resonating-Valence-Bond and Fractional Quantum Hall States, Phys. Rev. Lett. **59**, 2095 (1987).

[26] X. G. Wen, F. Wilczek, and A. Zee, Chiral spin states and superconductivity, Phys. Rev. B **39**, 11413 (1989).

[27] Y.-H. Chen, F. Wilczek, E. Witten, and B. Halperin, On anyon superconductivity, Int. J. Mod. Phys. B **3**, 1001 (1989).

[28] D.-H. Lee and M. P. A. Fisher, Anyon Superconductivity and the Fractional Quantum Hall Effect, Phys. Rev. Lett. **63**, 903 (1989).

[29] D.-H. Lee and C. L. Kane, Boson-Vortex-Skyrmion Duality, Spin-Singlet Fractional Quantum Hall Effect, and Spin-1/2 Anyon Superconductivity, Phys. Rev. Lett. **64**, 1313 (1990).

[30] R. B. Laughlin, Current stature of semioni pairing theory of high-tc superconductors, Int. J. Mod. Phys. B **5**, 1507 (1991).

[31] B. Bauer, L. Cincio, B. P. Keller, M. Dolfi, G. Vidal, S. Trebst, and A. W. W. Ludwig, Chiral spin liquid and emergent anyons in a Kagome lattice Mott insulator, Nat. Commun. **5**, 5137 (2014).

[32] Y.-C. He, D. N. Sheng, and Y. Chen, Chiral Spin Liquid in a Frustrated Anisotropic Kagome Heisenberg Model, Phys. Rev. Lett. **112**, 137202 (2014).

[33] S.-S. Gong, W. Zhu, and D. N. Sheng, Emergent chiral spin liquid: Fractional quantum Hall effect in a kagome Heisenberg model, Sci. Rep. **4**, 6317 (2014).

[34] Y.-C. He and Y. Chen, Distinct Spin Liquids and Their Transitions in Spin-1 /2 X X Z Kagome Antiferromagnets, Phys. Rev. Lett. **114**, 037201 (2015).

[35] S. Bieri, L. Messio, B. Bernu, and C. Lhuillier, Gapless chiral spin liquid in a kagome Heisenberg model, Phys. Rev. B **92**, 060407(R) (2015).

[36] A. Wietek, A. Sterdyniak, and A. M. Läuchli, Nature of chiral spin liquids on the kagome lattice, Phys. Rev. B **92**, 125122 (2015).

[37] S.-S. Gong, W. Zhu, L. Balents, and D. N. Sheng, Global phase diagram of competing ordered and quantum spin-liquid phases on the kagome lattice, Phys. Rev. B **91**, 075112 (2015).

[38] W.-J. Hu, W. Zhu, Y. Zhang, S. Gong, F. Becca, and D. N. Sheng, Variational Monte Carlo study of a chiral spin liquid in the extended Heisenberg model on the kagome lattice, Phys. Rev. B **91**, 041124(R) (2015).

[39] A. Szasz, J. Motruk, M. P. Zaletel, and J. E. Moore, Chiral Spin Liquid Phase of the Triangular Lattice Hubbard Model: A Density Matrix Renormalization Group Study, Phys. Rev. X **10**, 021042 (2020).

[40] W.-J. Hu, S.-S. Gong, and D. N. Sheng, Variational Monte Carlo study of chiral spin liquid in quantum antiferromagnet on the triangular lattice, Phys. Rev. B **94**, 075131 (2016).

[41] M. Hermele and V. Gurarie, Topological liquids and valence cluster states in two-dimensional SU(N) magnets, Phys. Rev. B **84**, 174441 (2011).

[42] P. Nataf, M. Lajkó, A. Wietek, K. Penc, F. Mila, and A. M. Läuchli, Chiral Spin Liquids in Triangular-Lattice SU(n) Fermionic Mott Insulators with Artificial Gauge Fields, Phys. Rev. Lett. **117**, 167202 (2016).

[43] J.-Y. Chen, S. Capponi, A. Wietek, M. Mambrini, N. Schuch, and D. Poilblanc, $SU(3)_1$ Chiral Spin Liquid on the Square Lattice: A View from Symmetric Projected Entangled Pair States, Phys. Rev. Lett. **125**, 017201 (2020).

[44] Y.-H. Zhang and A. Vishwanath, Electrical detection of spin liquids in double moiré layers, arXiv:2005.12925.

[45] Y. Kasahara, T. Ohnishi, Y. Mizukami, O. Tanaka, S. Ma, K. Sugii, N. Kurita, H. Tanaka, J. Nasu, Y. Motome *et al.*, Majorana quantization and half-integer thermal quantum Hall effect in a Kitaev spin liquid, Nature (London) **559**, 227 (2018).

[46] S. Bieri, C. Lhuillier, and L. Messio, Projective symmetry group classification of chiral spin liquids, Phys. Rev. B **93**, 094437 (2016).

[47] D. F. Schroeter, E. Kapit, R. Thomale, and M. Greiter, Spin Hamiltonian for which the Chiral Spin Liquid is the Exact Ground State, Phys. Rev. Lett. **99**, 097202 (2007).

[48] R. Thomale, E. Kapit, D. F. Schroeter, and M. Greiter, Parent Hamiltonian for the chiral spin liquid, Phys. Rev. B **80**, 104406 (2009).

[49] A. E. B. Nielsen, J. I. Cirac, and G. Sierra, Laughlin Spin-Liquid States on Lattices Obtained from Conformal Field Theory, Phys. Rev. Lett. **108**, 257206 (2012).

[50] M. Greiter, D. F. Schroeter, and R. Thomale, Parent Hamiltonian for the non-Abelian chiral spin liquid, Phys. Rev. B **89**, 165125 (2014).

[51] R. V. Mishmash, J. R. Garrison, S. Bieri, and C. Xu, Theory of a Competitive Spin Liquid State for Weak Mott Insulators on the Triangular Lattice, Phys. Rev. Lett. **111**, 157203 (2013).

[52] L. Balents, M. P. A. Fisher, and C. Nayak, Nodal liquid theory of the pseudo-gap phase of high-tc superconductors, Int. J. Mod. Phys. B **12**, 1033 (1998).

[53] Y.-M. Lu and A. Vishwanath, Theory and classification of interacting integer topological phases in two dimensions: A chern-simons approach, Phys. Rev. B **86**, 125119 (2012).

[54] T. Senthil and M. Levin, Integer Quantum Hall Effect for Bosons, Phys. Rev. Lett. **110**, 046801 (2013).

[55] Y.-F. Jiang and H.-C. Jiang, Topological Superconductivity in the Doped Chiral Spin Liquid on the Triangular Lattice, Phys. Rev. Lett. **125**, 157002 (2020).

[56] S.-S. Gong, W. Zhu, J. X. Zhu, D. N. Sheng, and K. Yang, Global phase diagram and quantum spin liquids in a spin-1/2 triangular antiferromagnet, Phys. Rev. B **96**, 075116 (2017).

[57] S. N. Saadatmand and I. P. McCulloch, Detection and characterization of symmetry-broken long-range orders in the

spin-1/2 triangular Heisenberg model, Phys. Rev. B **96**, 075117 (2017).

[58] Z. Zhu, D. N. Sheng, and A. Vishwanath, Doped Mott insulators in the triangular lattice Hubbard model, arXiv:2007.11963.

[59] H.-C. Jiang, Superconductivity in the doped quantum spin liquid on the triangular lattice, arXiv:1912.06624.

[60] X.-Y. Song, C. Wang, A. Vishwanath, and Y.-C. He, Unifying description of competing orders in two-dimensional quantum magnets, Nat. Commun. **10**, 4254 (2019).

[61] A. Kitaev, Anyons in an exactly solved model and beyond, Ann. Phys. **321**, 2 (2006).

[62] S. Moroz, A. Prem, V. Gurarie, and L. Radzihovsky, Topological order, symmetry, and Hall response of two-dimensional spin-singlet superconductors, Phys. Rev. B **95**, 014508 (2017).

[63] Y.-C. He, S. Bhattacharjee, R. Moessner, and F. Pollmann, Bosonic Integer Quantum Hall Effect in an Interacting Lattice Model, Phys. Rev. Lett. **115**, 116803 (2015).

[64] N. Read and D. Green, Paired states of fermions in two dimensions with breaking of parity and time-reversal symmetries and the fractional quantum Hall effect, Phys. Rev. B **61**, 10267 (2000).

[65] T. Senthil, J. B. Marston, and M. P. A. Fisher, Spin quantum Hall effect in unconventional superconductors, Phys. Rev. B **60**, 4245 (1999).

[66] W.-H. Ko, P. A. Lee, and X.-G. Wen, Doped kagome system as exotic superconductor, Phys. Rev. B **79**, 214502 (2009).

[67] T. Grover and A. Vishwanath, Quantum phase transition between integer quantum Hall states of bosons, Phys. Rev. B **87**, 045129 (2012).

[68] Y.-M. Lu and D.-H. Lee, Quantum phase transitions between bosonic symmetry-protected topological phases in two dimensions: Emergent QED_3 and anyon superfluid, Phys. Rev. B **89**, 195143 (2014).

[69] M. Barkeshli and J. McGreevy, Continuous transition between fractional quantum Hall and superfluid states, Phys. Rev. B **89**, 235116 (2014).

[70] F. Wu, T. Lovorn, E. Tutuc, and A. H. MacDonald, Hubbard Model Physics in Transition Metal Dichalcogenide Moiré Bands, Phys. Rev. Lett. **121**, 026402 (2018).

[71] Y. Tang, L. Li, T. Li, Y. Xu, S. Liu, K. Barmak, K. Watanabe, T. Taniguchi, A. H. MacDonald, J. Shan, and K. F. Mak, WSe2/WS2 moiré superlattices: A new Hubbard model simulator, arXiv:1910.08673.

[72] E. C. Regan, D. Wang, C. Jin, M. I. Bakti Utama, B. Gao, X. Wei, S. Zhao, W. Zhao, Z. Zhang, K. Yumigeta, M. Blei, J. D. Carlström, K. Watanabe, T. Taniguchi, S. Tongay, M. Crommie, A. Zettl, and F. Wang, Mott and generalized Wigner crystal states in WSe_2/WS_2 moiré superlattices, Nature (London) **579**, 359 (2020).

[73] L. Wang, E.-M. Shih, A. Ghiotto, L. Xian, D. A. Rhodes, C. Tan, M. Claassen, D. M. Kennes, Y. Bai, B. Kim, K. Watanabe, T. Taniguchi, X. Zhu, J. Hone, A. Rubio, A. Pasupathy, and C. R. Dean, Correlated electronic phases in twisted bilayer transition metal dichalcogenides, Nat. Mater. **19**, 861 (2020).